

A STATISTICAL ANALYSIS OF THE *EINSTEIN* NORMAL GALAXY SAMPLE.
I. SPIRAL AND IRREGULAR GALAXIESG. FABBIANO AND G. TRINCHIERI
Harvard-Smithsonian Center for Astrophysics
Received 1984 November 13; accepted 1985 March 18

ABSTRACT

Forty-eight spiral and irregular galaxies were observed with the *Einstein* observatory as part of the normal galaxy survey. In this paper we report the results of a statistical analysis of this sample. We find correlations of the X-ray luminosity with the optical (B), infrared (H), and radio continuum (1400 MHz) luminosities and to a lesser extent with the $B-H$ color. Our analysis shows that the primary correlations are those of the X-ray luminosity with the radio luminosity and with the blue luminosity and reveals different functional relationships. In particular, the correlation between X-ray and blue luminosity is not far from linear, while the one between X-ray and radio luminosity follows a power law with an exponent smaller than unity. We also find that early-type spirals (S0/a-Sbc) are underluminous in radio relative to their X-ray emission. These results lead us to conclude that the X-ray luminosity of spiral galaxies is largely connected with the blue-emitting Population I component of both the old disk and the spiral arms. A bulge component is, however, likely to be present in early-type spirals. The X-ray radio relationship suggests that X-ray sources are closely linked to the cosmic ray production. This link might be evolutionary, involving a supernova stage; or X-ray sources themselves might be the main producers of cosmic rays in spiral galaxies. The radio continuum emission would then be originating from both the old disk and the younger arm Population I components. Our results also suggest that larger and brighter spiral galaxies have larger magnetic fields and that the magnetic field intensity is related to the cosmic ray density, in agreement with the earlier conclusions of Parker.

Subject headings: galaxies: nuclei — galaxies: stellar content — galaxies: X-rays

I. INTRODUCTION

The study of field galaxies in X-rays has a manifold interest. It can help answer some of the open questions of "classical" galactic X-ray astronomy. For example, it can give some clues on the nature and origin of the galactic bulge X-ray sources (see Fabbiano, Trinchieri, and Macdonald 1984). It can reveal otherwise elusive phenomena, as best exemplified by the discovery of hot X-ray emitting gas ejected by the starburst nuclei of M82 (Watson, Stanger, and Griffiths 1984) and NGC 253 (Fabbiano and Trinchieri 1984). It can, most importantly, help explore a completely new dimension in the parameter space of the properties of normal galaxies. X-ray emission is probably one of the best observational tools for investigating the evolved component of the stellar population.

Most of the X-ray emission in the Milky Way is due to point-like X-ray sources, most likely compact accreting binaries containing one of the end products of stellar evolution: a neutron star, a black hole, or a white dwarf (e.g., Tananbaum and Tucker 1974). Supernova remnants and globular cluster sources also contribute to the X-ray emission (see review in Fabian 1981). X-ray observations with the *Einstein* satellite (Giacconi *et al.* 1979) of Local Group and other nearby galaxies (LMC, Long, Helfand, and Grabelsky 1981; SMC, Seward and Mitchell 1980; M31, Van Speybroeck *et al.* 1979; M33, Long *et al.* 1981; NGC 253, Fabbiano and Trinchieri 1984; M83, Trinchieri, Fabbiano, and Palumbo 1985) show that the X-ray emission of normal external galaxies can be similarly explained.

Although detailed models for explaining individual X-ray sources in the Milky Way and their evolution have been developed (see van den Heuvel 1980 and references therein), a study of the possible effects of different environments on such evolu-

tion has never been attempted. X-ray observations of a large number of galaxies of different morphology, luminosity, colors, etc., can help in setting the frame for such studies.

An *Einstein* X-ray survey of a sample of peculiar blue galaxies (Fabbiano, Feigelson, and Zamorani 1982) revealed correlations between the X-ray emission of these galaxies and both the optical (B) and the radio (1.4 GHz) emission. A tendency for galaxies with U excess to be stronger X-ray emitters than galaxies without U excess was also found. These results suggested a relationship between the young stellar Population I component and the integrated X-ray emission of late morphological type peculiar galaxies.

These conclusions were strengthened by the subsequent X-ray study of a small but representative sample of late-type normal spiral galaxies (Fabbiano, Trinchieri, and Macdonald 1984). Tight correlations were found in these galaxies between the 2 keV X-ray luminosity (l_X) and both the optical blue luminosity (l_B) and the radio continuum 1.4 GHz luminosity (l_R). No strong correlations were found with either the H (1.6 μ m) luminosity or the $B-H$ color, which are both good mass indicators (Aaronson, Huchra, and Mould 1979; Tully, Mould, and Aaronson 1982). These results suggested that the X-ray emission is not directly linked with the mass of spiral galaxies or the older stellar population, but with the stellar component contributing mostly to the blue light. Therefore even the so-called "Type II" component of the X-ray luminosity, or "bulge-type" sources (Giacconi 1974; van den Heuvel 1980), might be constituted by systems not much older than $\sim 10^9$ yr, belonging to the smooth disk population. While the correlation between l_X and l_B is linear, the correlation between l_X and l_R follows a flatter dependence ($l_X \propto l_R^{0.60 \pm 0.10}$). A Spearman partial rank test applied on l_X , l_B , and l_R showed that the l_X , l_R

and the l_x , l_B correlations are the two fundamental correlations between the three variables. The study of galaxies in X-rays might then also help in shedding some light on the debated origin of their radio emission (Hummel 1981; Klein 1982).

As remarked by Fabbiano, Trinchieri, and Macdonald (1984), all the above results were obtained using a relatively small sample of 14 galaxies, 11 of which are Sbc- or later-type galaxies. They needed to be confirmed by expanding the sample and by comparing galaxies of a wider variety of morphological types. This is the scope of the present paper and of the companion paper (Trinchieri and Fabbiano 1985), where the X-ray properties of elliptical galaxies are discussed. The X-ray sample we will use in these two papers is (with only a few additions) the sample of normal galaxies surveyed with *Einstein*, as published by Long and Van Speybroeck (1983, hereafter LVS). This sample consists of 29 elliptical and S0 and 48 spiral and irregular galaxies covering a wide range of morphological types and absolute magnitudes. We will search for correlations between the X-ray luminosity (l_x) and a large number of other galaxy properties, including the blue luminosity (l_B), the 1.4 GHz radio continuum luminosity (l_R), the H -band luminosity (l_H), the $B-H$ and $U-B$ colors, the morphological parameter T (de Vaucouleurs, de Vaucouleurs, and Corwin 1976), and the $H\ I$ luminosity.

Correlations between the optical and infrared parameters of spiral galaxies have been widely discussed in the literature. Correlations were found between the mass of spiral galaxies, as indicated by the $H\ I$ velocity dispersion, and B (Tully and Fisher 1977) and H (Aaronson, Mould, and Huchra 1980) luminosities, although with different slopes. The distance-independent $B-H$ color was then found to be a mass indicator (Tully, Mould, and Aaronson 1982). As summarized by Whitmore (1984), there has been a certain amount of debate on the nature of the parameters that can define spiral galaxies. Tully, Mould, and Aaronson (1982), in particular, conclude that one single parameter, total mass, can define the Hubble sequence for spiral galaxies. Rubin *et al.* (1982) instead conclude that two parameters are needed: the Hubble type and another parameter that could be either mass- or luminosity-related. In his recent work, Whitmore (1984) reanalyses all the various correlations between mass and optical-infrared galaxy parameters using a principal component analysis to find the dominant parameters. He concludes that two dimensions are needed to explain the observational properties of spiral galaxies. The two dimensions are identified by a combination of the blue luminosity and the radius at the 25th B mag arcsec $^{-2}$ isophote and of the $B-H$ color and the bulge-to-total light ratio. The first dimension is connected with the recent star formation rate and the second with the total mass of the galaxies.

In this paper we add two hitherto unused parameters, l_x and l_R , to the parameter space of spiral galaxies. We analyze the various relationships between these parameters and the optical-infrared parameters described above using the non-parametric Spearman partial rank correlation test (Kendall and Stuart 1976). In this way we seek to find the fundamental relationship, without introducing any assumption about the functional relationships between the variables. We then use regression techniques to find the functional relationships between the variables. Since our data include a number of upper limits (both in l_x and in l_R), statistical techniques that can handle censored data are used. These include the "detections and bounds" method (Avni *et al.* 1980) and some techniques recently developed and applied to astronomical problems by Schmitt (1985).

The sample is described and discussed in § II. The statistical analysis is described in detail in § III. The principal results are summarized in § IV and their implications discussed in § V.

II. THE SAMPLE

The sample we will use in this analysis is the sample of normal galaxies observed in X-ray with the *Einstein* Observatory as part of the Columbia Astrophysical Laboratory and Center for Astrophysics observing programs. The results of the observations are given in Table 4 of LVS, where the galaxies are listed, together with the morphological parameter T , the corrected face-on total blue magnitude, the $B-V$ and $U-V$ colors (all these parameters are from the *Second Reference Catalogue of Bright Galaxies*, de Vaucouleurs, de Vaucouleurs, and Corwin 1976), the distances and the 0.5–3.0 keV X-ray luminosity L_x . For details on the data analysis we refer to LVS. Some of the X-ray results of the LVS sample have also been published elsewhere (Van Speybroeck *et al.* 1979; Long, Helfand, and Grabelsky 1981; Long *et al.* 1981; Fabbiano, Feigelson, and Zamorani 1982; Fabbiano, Trinchieri, and Macdonald 1984; Stanger and Schwarz 1984). In this paper we analyze the data of the spiral and irregular sample. In the companion paper (Trinchieri and Fabbiano 1985), we analyze the elliptical sample.

To the LVS spiral sample we have added the three galaxies IC 342, IC 2574, and NGC 2613 (Fabbiano, Trinchieri, and Macdonald 1984). The X-ray fluxes of NGC 5253 and NGC 5907, detected in the same more recent analysis of the X-ray data, are also used instead of the upper limits of LVS. The resulting sample contains 48 S0/a, spiral, and irregular galaxies ($0 \leq T \leq 10$).

A thorough search in the literature allowed us to obtain radio continuum (1400 MHz), $H\ I$, and H -band data for most of the galaxies in the sample. The majority of the radio fluxes are from Hummel (1980). When the 1400 MHz flux was not available, we extrapolated measurements at 408 MHz (Harnett 1982) or at 2300 MHz (Dressel and Condon 1978), using a power-law spectrum with $\alpha = 0.7$ ($F_\nu \propto \nu^{-\alpha}$). Gioia, Gregorini, and Klein (1982) showed that the nonthermal radio continuum spectra of spiral galaxies all follow this universal slope. H -band (1.6 μm) infrared magnitudes for the spiral galaxies are from Aaronson (1977); Aaronson, Mould, and Huchra (1980); and Aaronson *et al.* (1982). All these H -band magnitudes were corrected using the growth curves of Aaronson, Huchra, and Mould (1979).

Of the 48 S0/a, spiral, and irregular galaxies, 39 have been detected in X-ray. For the other nine, the X-ray upper limits are used in the analysis. Radio measurements were available for 44 of the 48 galaxies, with 33 detections and 11 upper limits. H magnitudes were found in the literature for 35 of the 48 galaxies. The galaxies in the spiral and irregular sample and the integrated quantities used in this analysis are listed in Table 1. To be consistent with our previous work (Fabbiano, Feigelson, and Zamorani 1982; Fabbiano, Trinchieri, and Macdonald 1984), we used monochromatic fluxes (in units of mJy) and luminosities (in ergs s $^{-1}$ Hz $^{-1}$) for all the variables, except when color indices are involved. The 2 keV X-ray monochromatic fluxes and luminosities were all derived from the 0.5–3.0 keV band luminosities of LVS.

Although the sample is not statistically complete, it does not contain obvious selection biases, as the galaxies were chosen to cover a variety of morphological types and absolute magnitudes. Figure 1 shows the histograms of the blue magnitudes, the absolute magnitudes, and the morphological parameter T

TABLE 1
THE SPIRAL AND IRREGULAR GALAXIES SAMPLE

NGC	T	D^a	$\log l_R^b$	$\log l_H^b$	$\log l_B^b$	$\log l_X^b$	$B-H$
224	3	0.7	27.66	29.40	28.97	21.66	2.68
247	7	3.4	26.49	28.08	28.25	21.30	1.16
253	5	3.4	28.88	29.26	28.83	21.78	2.66
520	0	46.7	29.66	29.76	29.47	22.90	2.37
598	6	0.7	27.28	28.05	28.12	21.01	1.41
628	5	3.4	27.45	28.00	28.00	20.79	1.60
1073	5	26.4	<28.62	...	29.08	22.32	...
1097	3	24.5	29.65	...	29.54	23.18	...
1300	4	30.4	28.58	29.58	29.42	<22.65	1.99
1313	7	4.8	28.06	...	28.52	21.71	...
1350	2	29.3	<28.11	...	29.27	<22.63	...
1398	2	30.4	28.22	30.15	29.59	22.59	3.00
1559	6	20.5	29.36	29.04	29.20	22.66	1.18
LMC	9	0.05	28.15	20.59	...
2366	10	3.2	...	26.78	27.48	<20.60	-0.16
2403	6	3.2	27.58	28.52	28.43	21.47	1.82
2613	3	28.9	28.86	29.94	29.56	<22.80	2.54
2763	6	10.7	27.81	...	27.88	21.48	...
2775	2	19.3	<28.36	29.52	28.96	22.24	2.99
2835	5	10.7	27.89	28.56	28.41	<21.82	1.97
2841	3	12.0	28.22	29.49	29.06	22.08	2.67
2848	5	10.7	27.73	<21.42	...
2903	4	7.6	28.45	29.25	28.87	22.07	2.49
3031	2	3.2	27.68	29.36	28.85	22.35	2.86
3077	0	3.2	<26.80	27.65	27.64	20.37	1.62
3368	2	16.0	28.44	29.75	29.22	21.95	2.91
3593	0	16.0	28.45	...	28.64	22.03	...
3628	3	16.0	29.19	29.71	29.35	22.89	2.49
4236	8	3.2	<26.80	27.48	28.02	20.91	0.24
4244	6	5.0	<27.18	27.99	28.26	21.14	0.90
4449	10	5.0	27.82	28.04	28.32	21.50	0.88
4579	3	21.7	29.08	29.75	29.27	22.49	2.80
4594	1	19.3	28.92	30.39	29.80	23.04	3.06
4643	0	25.4	<28.59	29.71	29.04	<22.87	3.27
4753	0	22.7	<28.49	29.82	29.27	22.30	3.03
4826	2	5.0	27.43	29.05	28.54	21.56	2.85
5068	6	7.9	27.85	...	28.31	21.58	...
5078	1	7.9	27.72	21.22	...
5101	0	7.9	<27.57	...	27.90	<21.63	...
5236	5	7.9	29.10	29.53	29.39	22.46	1.94
5253	0	7.9	27.62	27.91	28.38	21.03	0.41
5457	6	7.2	28.72	29.37	29.25	22.24	1.88
5566	2	34.6	<28.86	...	29.51	<22.80	...
5907	5	18.4	28.67	29.59	29.22	22.24	2.50
6744	4	10.4	28.57	29.18	29.44	22.30	0.94
7793	8	3.4	26.80	28.00	28.04	21.30	1.48
IC 342	6	4.6	28.85	...	28.91	21.88	...
I2574	9	3.7	<27.04	27.18	27.67	20.77	0.36

^a Assumed distances in units of Mpc.

^b All monochromatic luminosities are in units of $\text{ergs s}^{-1} \text{Hz}^{-1}$.

for the 48 galaxies. Although galaxies relatively bright in apparent magnitude were observed, the distribution in absolute magnitude M_{B_T} and morphological type T are both representative of spiral galaxies, as can be seen, for example, by comparison with the *Revised Shapley-Ames Catalog* (Sandage and Tammann 1981).

For our subsequent analysis we divided the sample into two subsamples. The first one, which we call "early sample," includes all the galaxies with $0 \leq T \leq 4$. The second one, which we call "late sample," includes all the galaxies with $5 \leq T \leq 10$. This choice separates galaxies with $U-B > 0$ from those with $U-B < 0$. The two subsamples obtained this way contain an almost equal number of galaxies. Four Sbc galaxies are included in the "early sample." The inclusion of these in the "late sample" would not affect our results. The "early sample" includes seven galaxies with $T = 0$. Three of

these are S0/a, and four are non-Magellanic irregular. Of the latter, two, NGC 520 and NGC 5253, have fairly blue colors indicative of active star formation. This will be kept in mind when discussing the implications of our results for early-type spiral galaxies.

III. ANALYSIS

In this section we describe the statistical analysis of the LVS spiral and irregular sample of 48 galaxies ("total sample") and of the two subsamples of early morphological type ("early sample") and of late morphological type galaxies ("late sample") described in § II.

A variety of statistical methods was used to analyze the data, both nonparametric and parametric (for previous applications of some of these methods, see Tananbaum *et al.* 1983; Fabbiano *et al.* 1984; Fabbiano, Trinchieri, and Macdonald 1984). The nonparametric Spearman rank test was first used to inves-

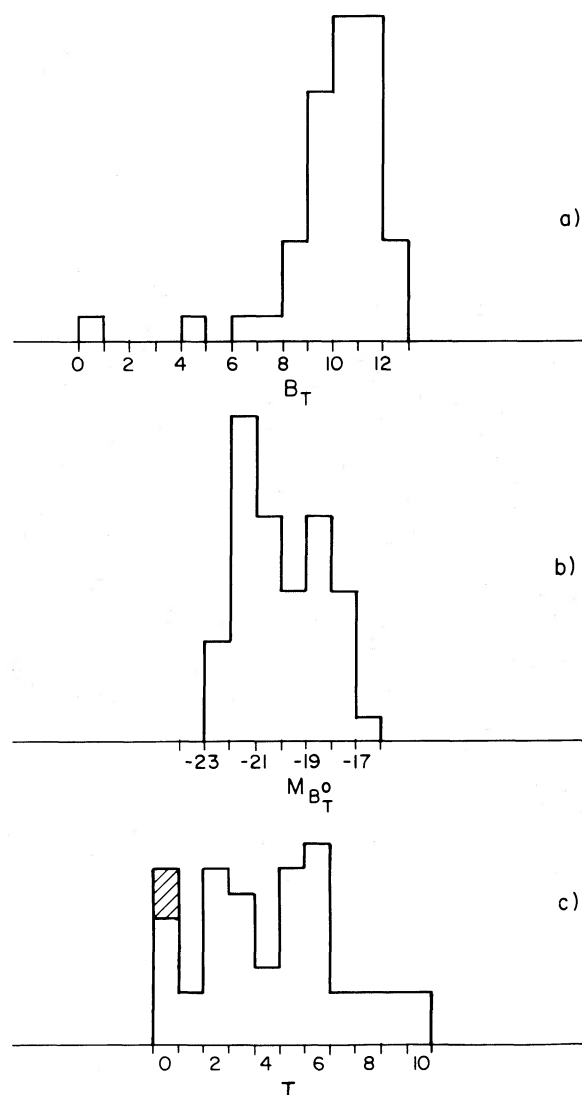


FIG. 1.—Histograms of (a) blue apparent magnitude B_T , (b) absolute magnitude $M_{B_T}^0$, and (c) morphological type T , for the 48 spiral and irregular galaxies of the sample. The shaded area in (c) identifies the two blue non-Magellanic irregulars NGC 520 and NGC 5253.

tigate the relationships between the X-ray emission (l_x), the blue light (l_B), the H -band emission (l_H), the radio continuum emission (l_R) and the $B-H$ color. This technique considers the rank of each variable ordered from largest to smallest values. In testing for the existence of associations between variables, rank correlation is superior to regression analysis because it does not require *a priori* assumptions about the functional form of any relationship. If bounds were present in the data (as is often the case), worst ranking correlation coefficients were also calculated. The results of this analysis are given in § IIIb. The Spearman partial rank test (Kendall and Stuart 1976) was then used to find which of the correlations are likely to derive from stronger primary correlations between some of the variables under examination.

To confirm some of the correlations and to establish functional dependences between the variables, a parametric analysis was then performed on the data (§ III d). We applied the “detections and bounds” method (Avni *et al.* 1980), which allows us to calculate best fit slopes with statistical uncertainties in the presence of upper limits. In cases in which bounds are present in both axes, the method developed by Schmitt (1985) was used to determine the best fit slopes.

a) *The Distribution of X-Ray Luminosities and of the X-Ray/Optical Flux Ratios*

Figures 2a–c show the histograms of the 0.5–3.0 keV X-ray luminosity L_x for the total sample and the two subsamples. The histograms of the 2 keV monochromatic X-ray flux to the B optical flux ratios f_x/f_B are shown in Figure 2d–f. Although the statistics are not such as to allow any strong conclusions, the histograms of L_x suggest that early-type spirals are brighter in X-rays than late-type spiral galaxies. The dependence of the X-ray luminosity on morphological type T inside each subsample is not, however, very well defined. Although there is a trend indicating that the X-ray luminosity decreases with increasing T , the scatter of L_x in each bin of T is quite large. This dependence of L_x on the morphological type could well be a consequence of the dependence of the optical luminosity on the morphological type, as already noted by LVS (see Fig. 9c of LVS), given the correlation between X-ray and B luminosities (§ III b). This is also exemplified by the histograms of f_x/f_B (Fig. 2d–f), where no difference can be seen between the two subsamples. They both have essentially the same distribution of f_x/f_B , peaked around 6.8×10^{-7} .

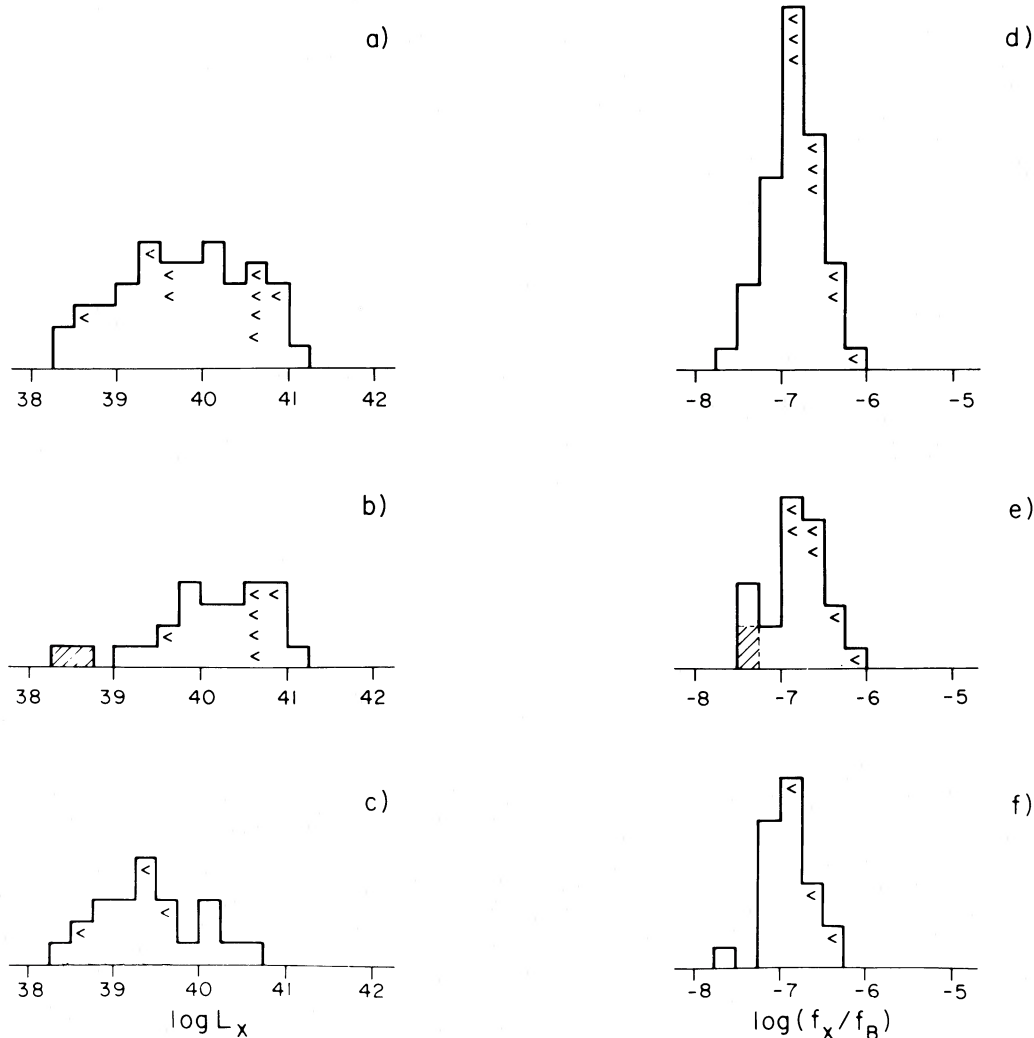


FIG. 2.—Histograms of $\log L_x$ for the (a) “total,” (b) “early,” and (c) “late” samples. (d–f) Analogous histograms of $\log(f_x/f_B)$. Shaded boxes in (b) and (e) represent the two blue non-Magellanic irregulars NGC 520 and NGC 5253. Their X-ray luminosities are the lowest in the “early” sample distribution.

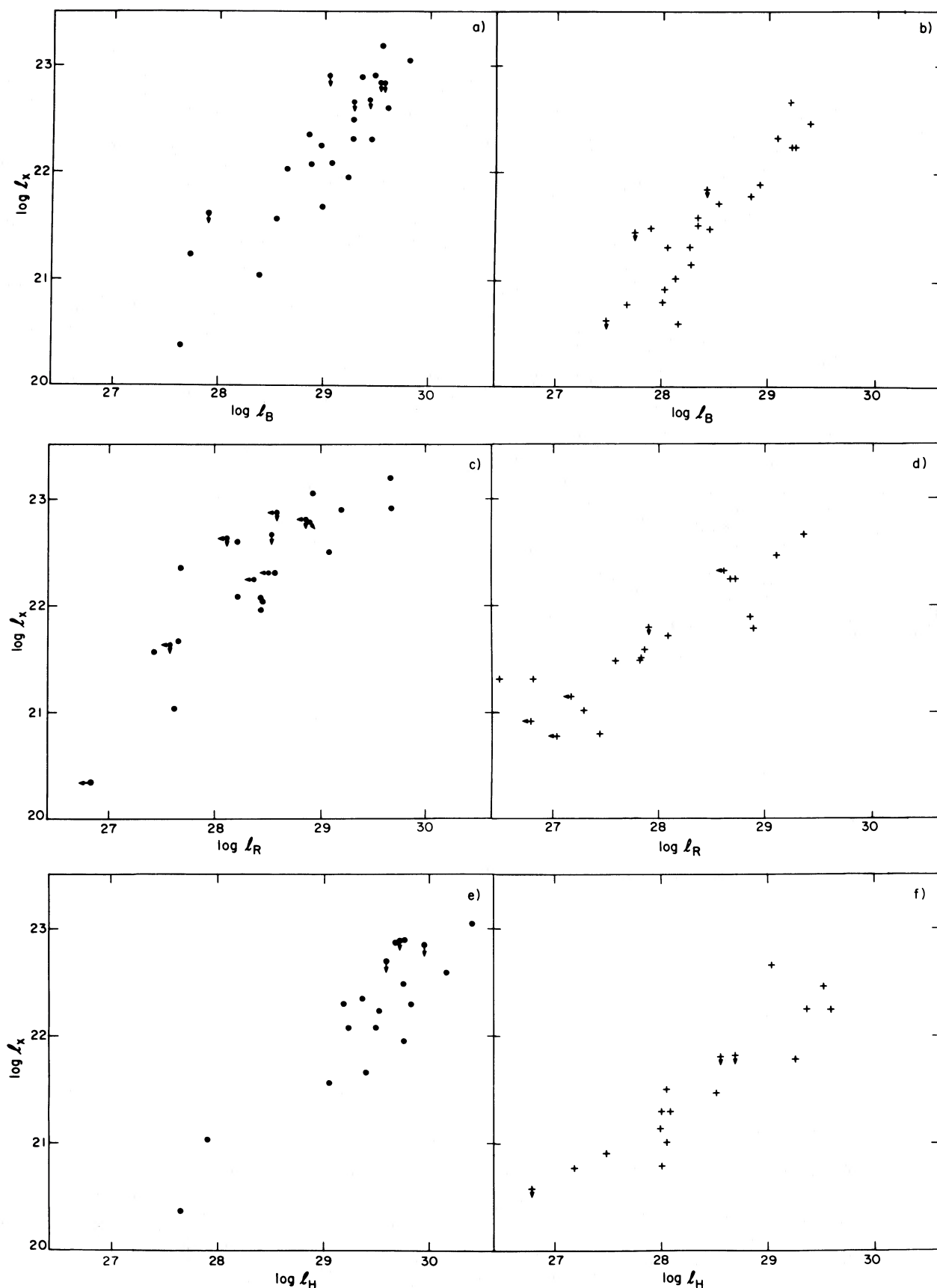


FIG. 3.—(a–b) Plots of the logarithm of the 2 keV monochromatic X-ray luminosity L_X vs. the logarithm of the blue luminosity l_B ; (c–d) of the logarithm of the 1.4 GHz radio luminosity l_R ; and (e–f) the logarithm of the H infrared luminosity l_H . All quantities are in units of $\text{ergs s}^{-1} \text{Hz}^{-1}$. Dots (left panels) identify “early sample” galaxies; crosses (right panels), “late sample” galaxies.

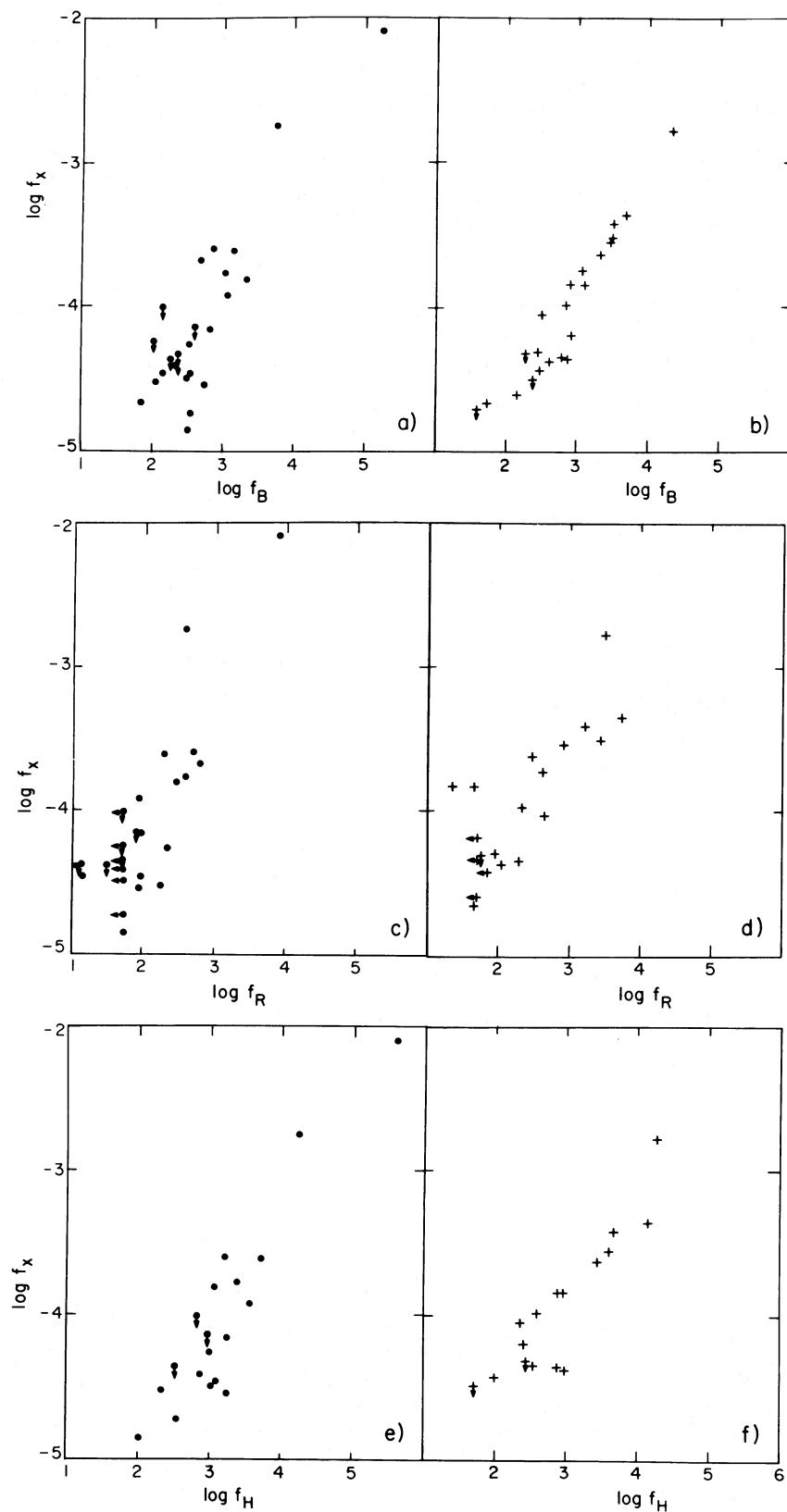


FIG. 4.—Plots of the logarithm of the 2 keV monochromatic X-ray flux f_x vs. (a–b) the logarithm of the blue flux f_B ; (c–d) the logarithm of the 1.4 GHz radio flux f_R ; and (e–f) the logarithm of the H infrared flux f_H . All quantities are in units of mJy. Dots (left panels) identify “early sample” galaxies, crosses (right panels), “late sample” galaxies.

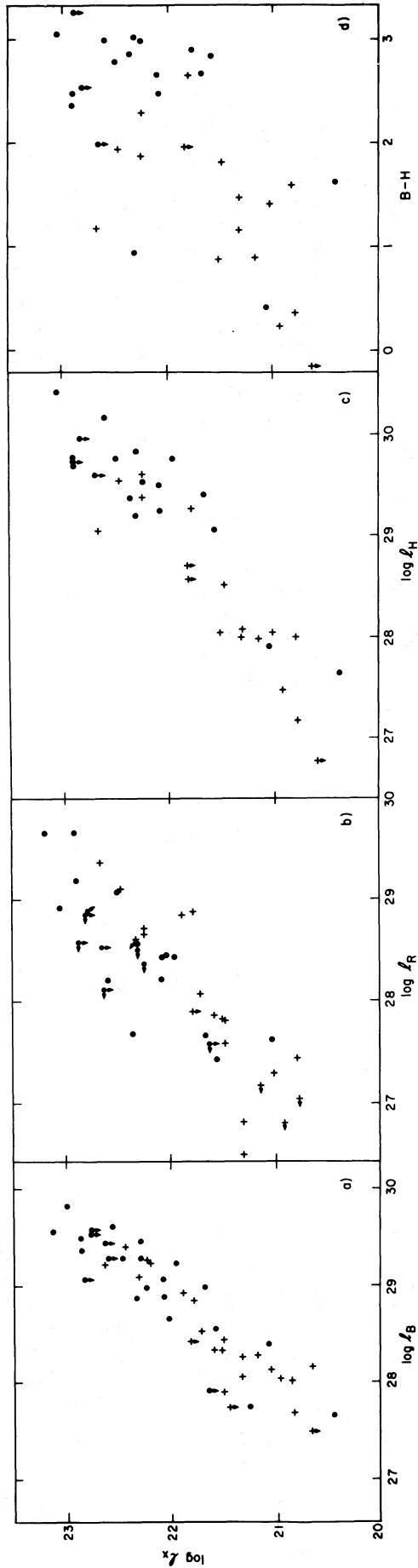


FIG. 5.—Log l_x vs. $\log l_B$, $\log l_R$, $\log l_H$, and $(B-H)$, for the "total sample." Dots identify "early sample" galaxies and crosses "late sample" galaxies.

TABLE 2
SPEARMAN RANK CORRELATION COEFFICIENTS AND PROBABILITIES (one-tailed)

CORRELATIONS	"EARLY SAMPLE" ($0 \leq T \leq 4$)						"LATE SAMPLE" ($5 \leq T \leq 10$)						"TOTAL SAMPLE" ($0 \leq T \leq 10$)									
	A		B		A		B		A		B		A		B		A		B			
	N	r_{SR}	P_{SR}	N	r_{SR}	P_{SR}	N	r_{SR}	P_{SR}	N	r_{SR}	P_{SR}	N	r_{SR}	P_{SR}	N	r_{SR}	P_{SR}	N	r_{SR}	P_{SR}	
I_X vs. I_B	19	0.88	$< 1 \times 10^{-6}$	25	0.32	$\sim 5\%$	20	0.87	$< 1 \times 10^{-6}$	23	0.98	$\leq 1 \times 10^{-6}$	39	0.93	$\leq 1 \times 10^{-6}$	48	0.45	$\sim 1 \times 10^{-3}$				
I_X vs. I_R	15	0.81	$\sim 2.5 \times 10^{-4}$	24	0.29	$\sim 10\%$	15	0.93	$< 1 \times 10^{-6}$	20	0.59	$\sim 2.5 \times 10^{-3}$	30	0.86	$\leq 1 \times 10^{-6}$	44	0.30	$\sim 2.5\%$				
I_X vs. I_H	16	0.75	$\sim 5 \times 10^{-4}$	19	0.41	$\sim 4\%$	14	0.87	$\sim 2.5 \times 10^{-5}$	16	0.76	$\sim 5 \times 10^{-4}$	30	0.86	$\leq 1 \times 10^{-6}$	35	0.55	$\sim 5 \times 10^{-4}$				
I_X vs. $B-H$	16	0.36	$\sim 10\%$	19	0.21	$\sim 35\%$	14	0.56	$\sim 4\%$	16	0.46	$\sim 5\%$	30	0.60	$\sim 5 \times 10^{-5}$	35	0.36	$\sim 2\%$				
f_X vs. f_B	19	0.80	$\sim 2.5 \times 10^{-5}$	25	0.71	$\sim 5 \times 10^{-5}$	20	0.94	$< 1 \times 10^{-6}$	23	0.95	$\leq 1 \times 10^{-6}$	39	0.86	$\leq 1 \times 10^{-6}$	48	0.87	$\leq 1 \times 10^{-6}$				
f_X vs. f_R	15	0.85	$\sim 5 \times 10^{-5}$	24	0.70	$\sim 5 \times 10^{-5}$	15	0.79	$\sim 5 \times 10^{-4}$	16	0.71	$\sim 1 \times 10^{-3}$	30	0.80	$< 1 \times 10^{-6}$	44	0.65	$\sim 1 \times 10^{-6}$				
f_X vs. f_H	16	0.79	$\sim 2.5 \times 10^{-4}$	19	0.81	$\sim 2.5 \times 10^{-5}$	14	0.81	$\sim 5 \times 10^{-4}$	16	0.83	$\sim 5 \times 10^{-5}$	30	0.75	$\sim 1 \times 10^{-6}$	35	0.74	$< 1 \times 10^{-6}$				

NOTE.—A, only detections; B, detections and bounds with worst ranking.

TABLE 3
SPEARMAN PARTIAL RANK CORRELATION COEFFICIENTS AND PROBABILITIES (one-tailed) THREE-VARIABLE TESTS (X, B, H, R)

SAMPLE	X, B, H						B, H, R						X, H, R						X, B, R								
	$\rho_{XB \cdot H}$		$\rho_{XH \cdot B}$		$\rho_{BH \cdot X}$		$\rho_{BH \cdot R}$		$\rho_{BR \cdot H}$		$\rho_{HR \cdot B}$		$\rho_{XR \cdot H}$		$\rho_{XR \cdot B}$		$\rho_{XR \cdot R}$		$\rho_{HR \cdot X}$		$\rho_{HR \cdot H}$		$\rho_{HR \cdot B}$		$\rho_{BR \cdot X}$		
	N	ρ	N	ρ	N	ρ	N	ρ	N	ρ	N	ρ	N	ρ	N	ρ	N	ρ	N	ρ	N	ρ	N	ρ	N	ρ	
"Early" ($0 \leq T \leq 4$)	16	0.64	16	0.56	15	0.71	0.43	0.10	13	0.63	0.64	0.64	0.64	15	0.69	0.50	0.09	0.09	0.09	0.09	0.09	0.09	0.09	0.09	0.09	0.09	0.09
"Late" ($5 \leq T \leq 10$)	14	0.75	$\sim 1.7 \times 10^{-3}$	14	0.47	$\sim 45\%$	12	0.86	0.58	$\sim 2.5 \times 10^{-4}$	11	0.57	0.79	0.79	0.79	0.79	0.79	0.79	0.79	0.79	0.79	0.79	0.79	0.79	0.79	0.79	0.79
"Total" ($0 \leq T \leq 10$)	30	0.73	$\sim 5 \times 10^{-6}$	30	0.61	$\sim 2.5 \times 10^{-4}$	27	0.81	0.50	$\sim 5 \times 10^{-3}$	24	0.61	0.72	0.72	0.72	0.72	0.72	0.72	0.72	0.72	0.72	0.72	0.72	0.72	0.72	0.72	0.72

NOTE.—Second line of each row gives probabilities.
^a Anticorrelation.

b) Nonparametric Analysis

i) Correlations between l_X and Other Quantities

Figure 3 shows the 2 keV monochromatic luminosity l_X plotted versus the monochromatic luminosities in the blue, l_B , in the H band, l_H , and in the radio at 1400 MHz, l_R , for the "early" and "late" samples. Analogous plots for the monochromatic fluxes are shown in Figure 4. The data for the "total" sample are shown in Figure 5, which also includes a plot of l_X versus the $B-H$ color. As can be seen from the figures, the data suggest correlations in all instances. This is especially true in the case of the "late sample," even considering the presence of bounds in the data. In the "early sample" more bounds are present, especially in the l_X versus l_R plot, making the situation less clear. As explained earlier in this section, we applied the Spearman rank correlation test to the data, to establish the confidence level of each correlation. This was done in two ways: first, correlation coefficients and probabilities that the correlation might arise from a random sample were calculated, using only the detections. Then, worst-case upper limits on the probabilities were calculated, ranking the objects with bounds in the most unfavorable way. This gives an upper limit on the probabilities corresponding to the most unlikely situation. The results are shown in Table 2, where the number of objects used in the test, the Spearman rank correlation coefficients, and the probabilities are given for each relationship. As can be seen from Table 2, all correlations are highly significant for the "late sample," and they are also significant in the "total sample." In the "early sample," an upper limit of 10% on the probability for the l_X versus l_R correlation is found, when the objects with bounds are given the worst ranking. The correlation, however, exists between the fluxes, and it is also confirmed by the parametric analysis (§ IIIc). The presence of correlations both in the fluxes and in the luminosities excludes the possibility of a distance bias in the data. The inclusion of the bounds in the analysis also allows us to avoid such an effect.

ii) Primary and Secondary Correlations

After the establishment of correlations of the 2 keV X-ray luminosity l_X with a number of other characteristic quantities of spiral galaxies, the question arises about which, if any, of these correlations are intrinsically valid, and which are the secondary results of other primary correlations. These questions can be answered with the Spearman partial rank correlation test (Kendall and Stuart 1976). A similar analysis was performed for a smaller sample of spiral galaxies by Fabbiano, Trinchieri, and Macdonald (1984).

We performed this test first on the four variables l_X , l_B , l_R , and l_H , in two different ways. We first selected groups of three variables in all possible independent combinations, and we derived the Spearman rank correlation coefficients for each correlation between two of the variables in each group of three. We only used the subset of detections common to all three variables each time. This test was performed on the total sample and on the two separate subsamples. The results are given in Table 3 and are shown in a graphic way in Figure 6a, where the primary correlations are indicated with a solid line. The primary correlations appear to be those between l_X and l_B , l_X and l_R , and l_B and l_H . We then performed the Spearman partial rank correlation test on the four variables l_X , l_B , l_R , and l_H simultaneously, using the subset of detections in all three variables l_X , l_R , and l_H . The number of objects used in this test

is necessarily smaller than the number in each of the three-variable tests. The results, however, are in agreement with those of the three-variable tests, as can be seen by inspection of Table 4.

The same procedure was then followed to analyze the correlations between l_X , l_B , l_H , and $B-H$. The results are given in Tables 5 and 6 and in Figure 6b. The principal correlations appear to be those between l_H and $B-H$, l_H and l_B , and l_X and l_B .

c) Parametric Analysis

i) Maximum Likelihood Analysis of the Correlations between l_X and Other Quantities

Inspection of Figures 3, 4, and 5 shows that the relationships between l_X and the other quantities could be represented by straight lines in the log-log plots. To find the slopes of these straight lines, we analyzed the data using the "detections and bounds" method by assuming a straight-line dependence between any two quantities and the points distributed with a Gaussian spread σ around this line. The basic underlying assumption of the "detections and bounds" method is that both detections and upper limits originate from the same parent population. In this way we included the upper limits in l_X in our analysis. Since there are a few radio upper limits, we also calculated the slopes of $\log l_R$ versus $\log l_X$, using the same method described above.

The results of the parametric analysis are given in Table 7. They confirm that all correlations are real at a good confidence level. The different functional relationships of the correlations between l_X and l_B and between l_X and l_R , noticed for a small sample of mainly late-type spiral galaxies by Fabbiano, Trinchieri, and Macdonald (1984), are confirmed. In particular, these different functional relationships are very clear in the "late sample" correlations. The correlations between l_X and l_H are also fitted with a power-law exponent smaller than unity. We obtained consistent results using the Schmitt (1985) method, which allows for the bounds in both variables to be considered simultaneously. In the case of bounds present in only one variable, this method is essentially the same as Avni *et al.*'s (1980) "detections and bounds" method. Using the Schmitt (1985) method, we confirm that the X-ray-radio correlations (bounds are present in both radio and X-ray data) are significant at a high significance level. The correlation coefficients are 0.86 ± 0.05 , 0.86 ± 0.09 , and 0.89 ± 0.04 for the "total," "early," and "late" samples respectively.

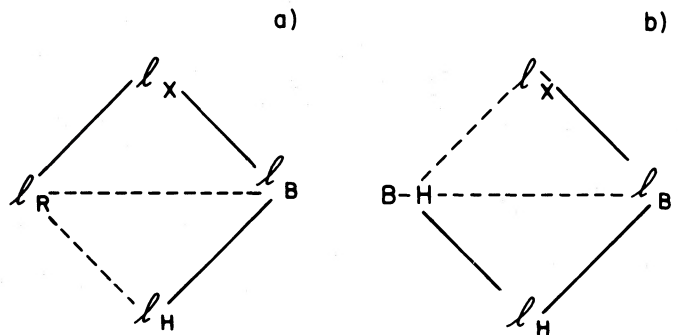


FIG. 6.—Schematic representation of the correlations between (a) l_X , l_B , l_R , and l_H , and (b) l_X , l_B , l_H , and $B-H$. Primary correlations are indicated by solid lines, secondary ones by dotted lines.

TABLE 4

SPEARMAN PARTIAL RANK CORRELATION COEFFICIENTS AND PROBABILITIES (one-tailed) FOUR-VARIABLE TEST (X, B, H, R)

Sample	N	$\rho_{XB \cdot HR}$	$\rho_{XH \cdot BR}$	$\rho_{XR \cdot BH}$	$\rho_{BH \cdot XR}$	$\rho_{BR \cdot XH}$	$\rho_{HR \cdot XB}$
"Early" ($0 \leq T \leq 4$)	13	0.40 ~10%	0.26 ~25%	0.46 ~7%	0.52 ~4%	0.27 ~25%	-0.12 a
"Late" ($5 \leq T \leq 10$)	11	0.76 ~1%	-0.29 a	0.58 ~5%	0.87 ~ 2×10^{-3}	0.02 ~40%	-0.07 a
"Total" ($0 \leq T \leq 10$)	24	0.56 ~ 2.5×10^{-3}	0.16 ~20%	0.53 ~ 5×10^{-3}	0.57 ~ 2.5×10^{-3}	0.16 ~20%	-0.22 a

NOTE.—Second line of each row gives probabilities.

^a Anticorrelation.

TABLE 5

SPEARMAN PARTIAL RANK CORRELATION COEFFICIENTS AND PROBABILITIES (one-tailed) THREE-VARIABLE TESTS ($X, B, H, B-H$)^a ("total sample" [$0 \leq T \leq 10$], $N = 30$)

$X, H, B-H$			$X, B, B-H$			$B, H, B-H$		
$\rho_{XH \cdot (B-H)}$	$\rho_{X(B-H) \cdot H}$	$\rho_{H(B-H) \cdot X}$	$\rho_{XB \cdot (B-H)}$	$\rho_{X(B-H) \cdot B}$	$\rho_{B(B-H) \cdot X}$	$\rho_{BH \cdot (B-H)}$	$\rho_{B(B-H) \cdot H}$	$\rho_{H(B-H) \cdot B}$
0.79 $< 1 \times 10^{-6}$	-0.44 b	0.76 ~ 1×10^{-6}	0.89 $< 1 \times 10^{-6}$	0.13 ~25%	0.13 ~25%	0.92 $\ll 1 \times 10^{-6}$	-0.70 b	0.85 $\ll 1 \times 10^{-6}$

NOTE.—Second line gives probabilities.

^a The results for the three variables X, B, H are given in Table 2.^b Anticorrelation.

TABLE 6

SPEARMAN PARTIAL RANK CORRELATION COEFFICIENTS AND PROBABILITIES (one-tailed) FOUR-VARIABLE TEST ($X, B, H, B-H$) ("total sample" [$0 \leq T \leq 10$], $N = 30$)

$\rho_{XB \cdot H(B-H)}$	$\rho_{XH \cdot B(B-H)}$	$\rho_{X(B-H) \cdot BH}$	$\rho_{BH \cdot X(B-H)}$	$\rho_{B(B-H) \cdot XH}$	$\rho_{H(B-H) \cdot XB}$
0.61 ~ 2.5×10^{-4}	-0.20 a	0.41 -1%	0.75 ~ 2.5×10^{-6}	-0.75 a	0.96 $\ll 1 \times 10^{-6}$

NOTE.—Second row gives probabilities.

^a Anticorrelation.

TABLE 7

"DETECTIONS AND BOUNDS" LINEAR FIT COEFFICIENTS AND DISPERSION

Y^a	X^a	"EARLY SAMPLE" ($0 \leq T \leq 4$)			"LATE SAMPLE" ($5 \leq T \leq 10$)			"TOTAL SAMPLE" ($0 \leq T \leq 10$)		
		A	B	σ	A	B	σ	A	B	σ
$\log I_X$	$\log I_B$	1.05 ± 0.10	-8.3	0.30	1.08 ± 0.10	-9.2	0.25	1.08 ± 0.07	-9.2	0.25
$\log I_X$	$\log I_R$	0.69 ± 0.11	+2.6	0.30	0.53 ± 0.08	+6.8	0.25	0.65 ± 0.09	+3.6	0.35
		0.81 ± 0.15^b			0.59 ± 0.08^b			0.72 ± 0.7^b		
$\log I_X$	$\log I_H$	0.87 ± 0.10	-3.5	0.30	0.74 ± 0.12	+4.9	0.30	0.74 ± 0.06	+0.4	0.30
$\log I_R$	$\log I_X$	1.05 ± 0.10	+5.0	0.40	1.45 ± 0.20	-3.5	0.45	1.15 ± 0.08	+2.9	0.45
		0.91 ± 0.13^b			1.34 ± 0.15^b			1.03 ± 0.10^b		
$\log f_X$	$\log f_B$	$0.90^{+0.08}_{-0.10}$	-6.6	0.30	$0.83^{+0.03}_{-0.04}$	-6.4	0.15	0.84 ± 0.05	-6.4	0.25
$\log f_X$	$\log f_R$	$1.05^{+0.15}_{-0.25}$	-6.3	0.40	0.5 ± 0.15	-5.1	0.30	0.73 ± 0.10	-5.6	0.40
$\log f_X$	$\log f_H$	0.83 ± 0.13	-6.6	0.25	0.65 ± 0.12	-5.8	0.20	0.75 ± 0.90	-6.3	0.40

^a $Y = AX + B$ with a dispersion σ around the straight line.^b These values of the best fit slopes were obtained by taking into account all the bounds present in the data (radio and X-ray) with the Schmitt 1985 method.

ii) *The X-Ray-Radio Correlation in the "Early" and "Late" Samples*

The log l_X versus log l_R plot (Fig. 3c) for the "early sample", containing a larger number of bounds, shows a significantly larger scatter. The plot also suggests (see also best fit line in Table 7) that early-type spirals have relatively less radio emission for a given l_X than late-type spirals. We can investigate this effect further by examining the distribution of the residuals of both subsamples about the best fit line of the l_X versus l_R relationship for the "late sample." This is shown in Figure 7a. It is obvious that the two distributions are different, with the early sample showing an "excess" of l_X with respect to the best fit line for late-type galaxies (negative residuals). The only point with a large positive residual is NGC 5253, which is a very blue non-Magellanic irregular galaxy and therefore different from early-type spirals. A Kolmogoroff-Smirnoff test on the distributions of residuals for the detections only gives a probability of $\sim 1.5\%$ (one-sided) that the two distributions originate from the same parent population, if the residual of NGC 5253 is not used. A Kolmogoroff-Smirnoff test on the two distributions obtained using the upper limits in such a way as to minimize the differences gives a probability of $\sim 5\%$. Two-sample tests that take into account the limits in the distributions of residuals (Schmitt 1985) give probabilities in the $\sim 3\%$ to $\sim 1\%$ range. Therefore, the distribution of the residuals of the "early sample" with respect to the best fit for the l_X , l_R relationship for the "late sample" galaxies indicates an "excess" of l_X for the same l_R .

However, galaxies of different morphological types have different disk-to-bulge ratios (Simien and de Vaucouleurs 1983; Kent 1984). The bulge can contribute a significant amount to the optical emission of early-type spiral galaxies. Since l_X is

well correlated with l_B , we can assume that similar disk-to-bulge ratios apply to the X-ray luminosities. If we correct the observed l_X by the disk-to-bulge ratio and we use only "disk" X-ray luminosities, we notice that the distribution of residuals of the "early sample" becomes consistent with that of the "late sample" (Fig. 7c). A Kolmogoroff-Smirnoff test on the two distributions of Figures 7b and 7c gives a probability of $\sim 30\%$ (one-sided) that the two distributions derive from the same parent population. Similar values are obtained with the two-sample tests of Schmitt (1985).

iii) *Joint Linear Regression Analysis on l_X , l_B , and l_R for the "Late Sample"*

By using the "detections and bounds" method, we also performed a joint linear regression analysis (G. Zamorani 1984, private communication) to find the functional dependence between the X-ray luminosity l_X and the blue and radio luminosities l_B and l_R . Given the uncertainties on the radio-X-ray relationship in the "early sample," we calculated a joint linear regression only for "late sample" galaxies. The result is the following:

$$\log l_X = (0.75 \pm 0.20) \log l_B + (0.38 \pm 0.10) \log l_R + 22.3 .$$

The errors are the 1σ uncertainties on each slope, considered as the interesting parameter. This shows that, for a constant value of l_B , the relationship between l_X and l_R is of the form $l_X \propto l_R^{0.4}$. For a constant value of l_R , the relationship between l_X and l_B is of the form $l_X \propto l_B^{0.8}$, and possibly consistent with a linear relationship, within the statistical uncertainties.

The nonparametric analysis has shown that there is no strong direct correlation between l_B and l_R , while there are strong correlations between l_X and both variables. On a first-order approximation, we could then consider l_B and l_R to be independent variables. In this case the "detections and bounds" joint linear regression coefficients directly give us the functional relationship between l_X and these other two variables. Note that these coefficients are not very different from those derived for the two correlations independently (see Table 7).

d) *Other Correlations*

We searched for correlations with other quantities, like the total neutral hydrogen content and the $U-B$ color. We found a possible relationship of l_X with the H I luminosity, although with a very large scatter. Part of the scatter is due to "late sample" galaxies having systematically lower values of X-ray-to-H I flux ratio relative to "early sample" galaxies. This probably just reflects the fact that early-type spiral galaxies have a lower neutral hydrogen content (e.g., Faber 1981). The plot of the X-ray-to-optical (blue) flux ratio f_X/f_B versus the $U-B$ color is shown in Figure 8. Essentially no correlations are found in either sample. A trend of increasing f_X/f_B with decreasing $U-B$ is, however, observed if blue peculiar galaxies (Fabbiano, Feigelson, and Zamorani 1982) are added to the "late sample" galaxies.

e) *Potential Biases and Discussion of the Correlations*

Although the definitive answer will require a statistically well-defined sample of galaxies all observed, and detected, in radio, H, B, and X-rays, it is unlikely that the results of our nonparametric multivariate analysis (§ IIIb) could be due to biases resulting from discarding the upper limits in the Spear-

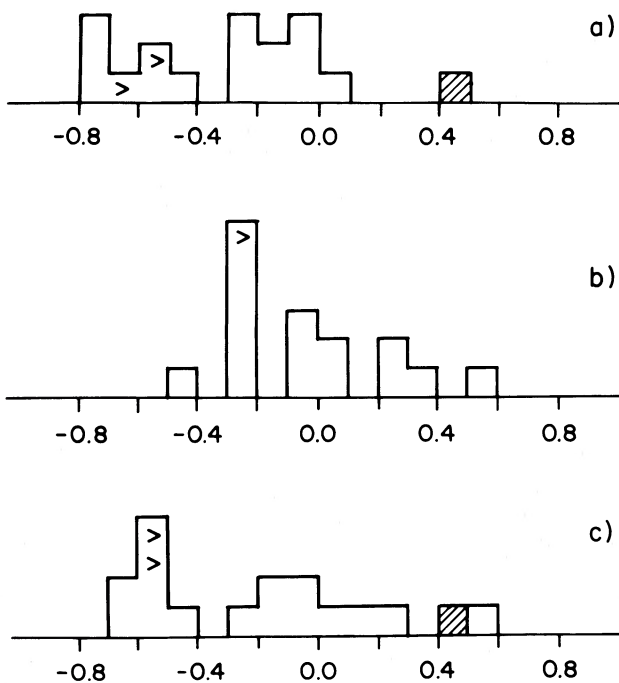


FIG. 7.—Histograms of differences between predicted and observed l_X for (a) "early" and (b) "late" sample galaxies. The predicted l_X were derived from the best fit "detections and bounds" line of Table 7 for the "late sample" galaxies. (c) Histogram obtained after correcting for disk to bulge ratios (see text). The shaded box in (a) and (c) represents the blue non-Magellanic irregular NGC 5253.

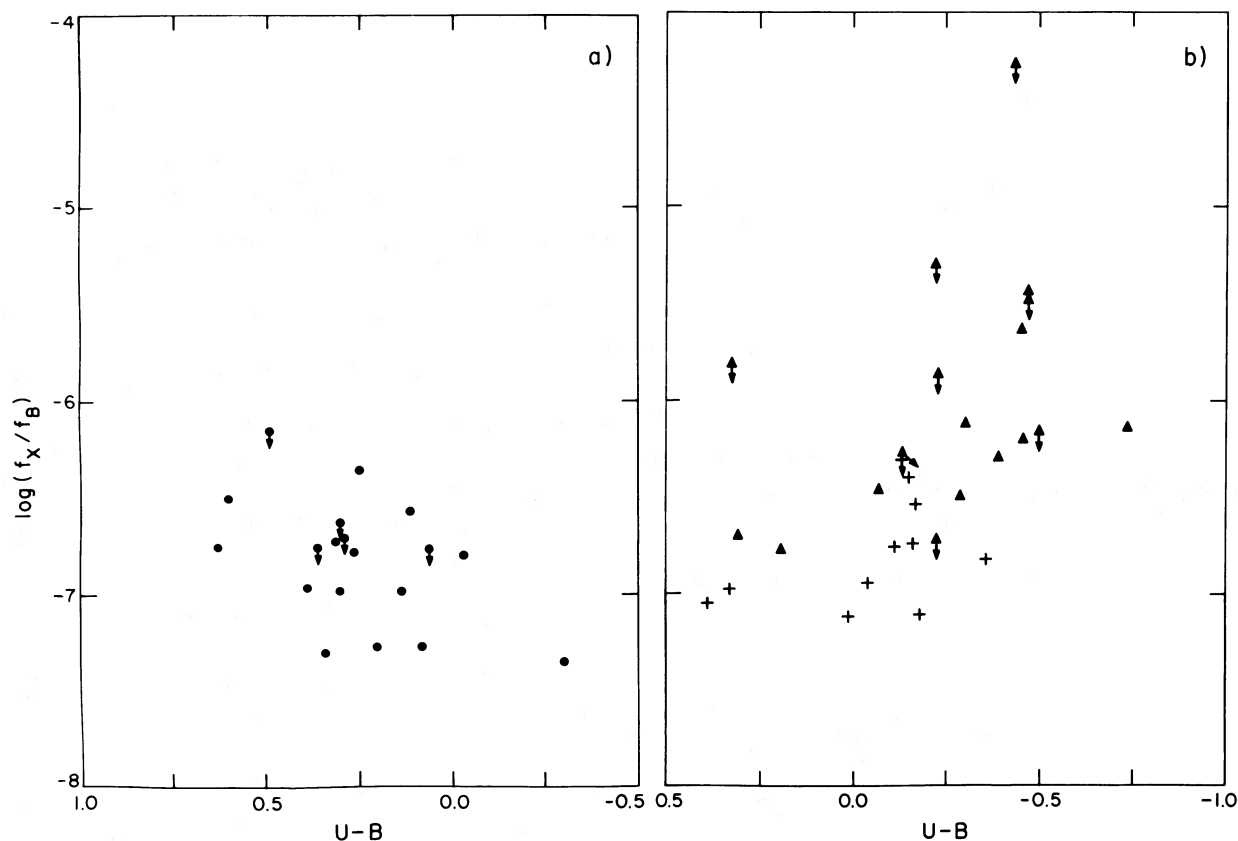


FIG. 8.—Plot of $\log(f_X/f_B)$ for (a) “early” and (b) “late” sample galaxies. Triangles in (b) represent the peculiar galaxies of Fabbiano, Feigelson, and Zamorani (1982).

man partial rank correlation test. This is especially true for the “late sample,” where only few galaxies have limits. These limits are all consistent with the distribution of the detections and the best fit relationships (see § IIIc). Given the way the limits and the detections are distributed, excluding the galaxies with limits does not result in detecting only very bright, or very dim, objects. The “detection only” sample is representative of normal galaxies as a whole. Also, the various subsamples used in the three- and four-variable tests are of necessity slightly different. The results we obtain are, however, consistent.

In the l_X , l_R , and l_B test for the “late sample,” in particular, five galaxies were discarded of the available 20 galaxies with radio measurements. Four of them have radio upper limits, and one has an X-ray upper limit. Excluding the X-ray upper limit, and giving the four radio upper limits the worst possible ranking, still results in the l_B , l_R relationship being the likely by-product of the other two more fundamental relationships between the three variables. Only if we position the X-ray upper limit at the lowest possible place in the l_X distribution does the l_X , l_R relationship become less likely than the l_B , l_R correlation. But this distribution of the limits is extremely unlikely. If we distribute, still conservatively but more realistically, the upper limits with the worst possible rank consistent with the dispersion of each diagram, the result still is that the l_R , l_B relationship is likely to be a secondary one.

Further confirmation of this result derives from the parametric analysis of the data with the Schmitt (1985) method (see § IIIc). The linear regression correlation coefficients for the l_B , l_R correlation are typically smaller than those for the l_X , l_B and

l_X , l_R correlations, in agreement with the results of the Spearman partial rank correlation test.

Even fewer galaxies (three in the “early sample” and two in the “late”) were discarded in the l_X , l_B , l_H , $B-H$ tests because of upper limits in l_X . These limits were again all consistent with the distribution of detections. The scatter of points in all the correlations is typically ≥ 0.3 in the log (see § IIIc and Table 7), too large for statistical and instrumental errors in the measurements to affect our results. Internal reddening in the galaxies should typically affect the B more than the H magnitudes, adding possible scatter to the l_X , l_B correlation. This is, however, already tighter than the l_X , l_H correlation. Removal of a possible reddening would then make our results even stronger. The X-ray luminosity should not be strongly affected by an internal absorption column, since the X-ray emission is likely to be dominated by hard X-ray sources (see Fabbiano, Feigelson, and Zamorani 1982 and Trinchieri, Fabbiano, and Palumbo 1985). Any very soft component that could be affected by the galaxy aspect and reddening, like the jetlike outflow seen in the HRI image of NGC 253 (Fabbiano and Trinchieri 1984), would contribute marginally to the values of l_X used in this paper, which are derived mainly from IPC observations. The IPC has a harder energy response than the HRI (Giacconi *et al.* 1979).

Although the galaxies in the sample are representative of normal spirals, some of them might have an X-ray-bright nuclear region, due either to starburst (NGC 253, Fabbiano and Trinchieri 1984; M83, Trinchieri, Fabbiano, and Palumbo 1985) or nonthermal activity (M81, Elvis and Van Spiebroeck

1982; M51, Palumbo *et al.* 1985). The X-ray luminosity of these sources, however, is typically smaller than the total integrated X-ray emission. The presence of such a source might introduce some scatter in the correlations. In the case of a nonthermal source we would expect this to affect equally the l_X , l_B , and the l_X , l_H correlations, since the nucleus will not contribute significantly either to l_B or to l_H . In the case of a starburst nuclear region, we would expect more scatter to be introduced in the l_X , l_B correlation than in the l_X , l_H correlation, since l_B would be affected more by dust in the nuclear region than l_H . Removal of all these effects would either not affect our results or give an even stronger l_X , l_B correlation and a weaker l_X , l_H correlation.

The results of our analysis are also consistent with those of Whitmore (1984), who showed that there is an intrinsic difference between B and H (or $B-H$) in spiral galaxies.

IV. SUMMARY OF RESULTS

The results of § III can be summarized as follows:

a) The X-ray 0.5–3.0 keV luminosities of spiral galaxies are in the range of $\sim 10^{38}$ to $\sim 10^{41}$ ergs s^{-1} . Comparison of the distributions of X-ray luminosities suggests that early-type spiral galaxies tend to be brighter X-ray emitters than later type galaxies. The distribution of X-ray-to-optical (blue) flux ratios are, however, similar and peaked around $f_X/f_B \sim 6.8 \times 10^{-7}$.

b) The X-ray luminosity l_X is correlated with the blue optical luminosity l_B , the radio continuum luminosity l_R , and the infrared H -band luminosity l_H in all three samples: the “early” ($0 \leq T \leq 4$, S0/a–Sbc), the “late” ($5 \leq T \leq 10$, Sc–Im), and the “total” ($0 \leq T \leq 10$, S0/a–Im) samples. A correlation of l_X with the color $B-H$ is also present in the “total” sample. The Spearman partial rank test shows that the primary correlations are

- (1) l_X with l_B and l_R ,
- (2) l_H with l_B and $B-H$.

Our results suggest that the radio luminosity l_R is not directly related to the optical luminosity l_B , and the X-ray luminosity l_X is not directly related to either the H -band luminosity l_H or the $B-H$ color.

c) These relationships are not all linear and clearly differ from each other. The correlation between l_X and l_B has a slope not far from linear. However, the correlations between l_X and l_R or l_H can be fitted with a power law with exponent smaller than unity.

d) The “early sample” ($0 \leq T \leq 4$) galaxies are not as strongly correlated with l_B as the “late sample” ones (see Tables 3 and 4). They are also underluminous in radio relative to their X-ray emission by comparison with the “late sample” ($5 \leq T \leq 10$) galaxies. After correcting l_X for the optical disk-to-total light ratio, we find that the relationship between the disk components of l_X of the “early sample” galaxies and their radio emission is in closer agreement with that of “late sample” galaxies. This correction, however, assumes that the X-ray luminosity is composed of a disk component and a bulge component, and that the X-ray luminosity of each component is proportional to their optical luminosity.

e) No correlations of the f_X/f_B flux ratio with the $U-B$ color is observed in normal spiral galaxies. The data are, however, consistent with the trend observed in bluer peculiar galaxies.

V. DISCUSSION

In the previous sections we have summarized the main results of our analysis of the LVS spiral and irregular galaxy sample. Here we will discuss the implications of these results for the nature of the X-ray emission of these galaxies, for the nature of their radio emission, and for the relationship of X-ray and radio emission to other galaxy properties.

a) *The Disk and Arm Component of the X-Ray Emission of Spiral and Irregular Galaxies*

The multivariate nonparametric statistical analysis of the LVS spiral and irregular galaxy sample presented in this paper overall confirms and strengthens our previous results (Fabbiano, Trinchieri, and Macdonald 1984) of a strong link between the X-ray emission and the blue-emitting Population I component (represented by l_B), rather than galaxy mass or the older stellar component (represented by l_H or $B-H$, see Whitmore 1984, and references therein). The results of the parametric analysis can also be understood in this picture. Both in the “total” and in the “late” sample of disk-dominated galaxies, the X-ray luminosity is linearly correlated with the luminosity in the blue ($l_X \propto l_B$). The relationship between l_X and the H -band luminosity is instead one of the form $l_X \propto l_H^{0.74}$. Aaronson, Huchra, and Mould (1979) found the following relationships between galaxy mass M , l_B , and l_H in spiral galaxies: $M \propto l_H$ and $M/l_B \propto l_H^{1/4}$, which combined give $l_B \propto l_H^{0.75}$. The strong proportionality between l_X and l_B would then result in the observed relationship between l_X and l_H . These results, as already discussed in Fabbiano, Trinchieri, and Macdonald (1984), have an impact on our knowledge of the nature and evolution of galactic X-ray sources.

The X-ray luminosity of the Milky Way is dominated by bright X-ray sources belonging to one of two types (see, e.g., van den Heuvel 1980). “Type I” sources are massive binary systems belonging to the extreme young Population I of the spiral arms. They are composed of a massive bright early-type star and a compact companion, either a neutron star or a black hole. The nature and evolution of these sources is fairly well understood. “Type II” sources, by contrast, are binary systems composed of a low-mass star and a more massive compact companion, most likely a neutron star. They are found evenly distributed in the region within $\pm 30^\circ$ of Galactic longitude. Among them are the very bright “GX” sources found in early rocket flights. They are likely to contribute most of the total X-ray emission of the Milky Way (Gursky 1976). The nature and evolution of these low-mass binary X-ray sources is still one of the unsolved problems of X-ray astronomy. It was originally suggested that they may belong to a Galactic bulge component (e.g., Giacconi 1974). Speculations on their origin have included capture of low-mass stars by neutron stars in the Galactic bulge (van den Heuvel 1980), remnants of disrupted globular clusters (Grindlay 1984), or the evolved remnants of native low-mass binary systems (e.g., Gursky 1976; Rappaport, Joss, and Webbink 1982; Nomoto 1984).

Assuming that disk-dominated spiral galaxies have an X-ray source population similar to that of the Milky Way (itself an Sc system, Hodge 1983), our result of an association between X-ray emission and the blue-emitting Population I component suggests that the low-mass binary X-ray sources belong to the disk population and not to a Population II component. This view is also strengthened by the recent imaging study of M83 (Trinchieri, Fabbiano, and Palumbo 1985), a galaxy morpho-

logically similar to the Milky Way (e.g., Jensen, Talbot, and Dufour 1981), and of M51, another Sbc galaxy (Palumbo *et al.* 1985). Comparison of the X-ray and the blue surface brightness profiles of these galaxies convincingly associates the bulk of the X-ray luminosity, and the low-mass binary component in particular, with the exponential galactic disk component, rather than with a spheroidal bulge, or a predominant spiral arm young Population I component.

As discussed in Fabbiano, Trinchieri, and Macdonald (1984), the association of the X-ray emission with the Population I component argues against a capture origin (van den Heuvel 1980) for the low-mass binary sources. The disrupted globular cluster scenario (see Grindlay 1984, and references therein) is not directly compatible with our results either. In this picture low-mass X-ray binaries would form by capture in globular clusters which are then disrupted by the interaction with the giant molecular clouds of the galactic plane. Only if the stellar population of the globular cluster progenitors belongs to the old Population I that composes the smooth disks, as might be suggested by the high metallicity (Grindlay 1984), could one plausibly explain the correlation of l_X with l_B and the lack of correlation of l_X with Population II (mass) indicators.

Evolutionary scenarios in which low-mass X-ray binaries evolve from native binary systems belonging to the smooth disk old Population I would be in agreement with our results. A first such scenario was discussed by Gursky (1976), who also suggested a link between these X-ray sources and Type I supernova events in the galactic disk. More detailed recent models suggest evolutive paths for native disk binary systems involving either direct core collapse of the more massive member to a neutron star, or collapse triggered by accretion onto a white dwarf with or without an associated Type I supernova event (Webbink, Rappaport, and Savonije 1983; Canal, Isern, and Labay 1982, 1984; Nomoto 1984).

b) *The X-Ray Emission of Early Spirals ($0 \leq T \leq 4$) and the X-Ray Sources of the Spheroidal Bulges*

Although "type II" or "galactic bulge" sources were seen in the previous section to belong mostly to the disk population, our results strongly suggest that another class of X-ray sources is associated with the spheroidal bulge population. The correlations between l_X and optical and infrared parameters (l_B , l_H) of the "early" ($0 \leq T \leq 4$) and "late" ($5 \leq T \leq 10$) sample galaxies are similar overall. The correlation between l_X and l_B , however, is less tight in the "early sample," and there is some indication of a better correlation between l_X and l_H than in the "late sample" (see Tables 3 and 4). There is also an indication of a steeper correlation between these two quantities than in the "late sample" (see Table 7). However marginal, this could suggest a link between some of the X-ray emission of these galaxies and the red-emitting stellar population. Moreover, a striking difference is apparent in the relationship between l_X and the radio continuum luminosity l_R , in the sense that early-type spirals are underluminous in radio relative to their X-ray emission. As discussed in § III, this difference might indicate the presence of a significant X-ray bulge component in early-type spirals, which are optically dominated by their bulges ($\sim 80\%$ – 40% of the light for $0 \leq T \leq 2$, Simien and de Vaucouleurs 1983; Kent 1984).

Thermal X-ray emission from cooling flows (Nulsen, Stewart, and Fabian 1984; White and Chevalier 1984) could be present in the bulges of early-type spiral galaxies. However, the

X-ray emission of bulges is likely to be dominated by discrete sources, as clearly shown by the high-resolution *Einstein* images of M31, an Sb galaxy (Van Speybroeck *et al.* 1979). The X-ray luminosities of the M31 bulge sources ($L_X \approx 10^{37}$ ergs s^{-1}) suggest that they are accreting close binary systems. Some of these sources cluster in a small region in the inner core of the galaxy, and a similar number are distributed throughout the bulge. Statistical considerations similar to those of Lightman and Grindlay (1982) show that capture of a low-mass star by a neutron star could account for the inner core sources, but not for the outer bulge sources, given the larger volume (and therefore smaller densities) involved. The same evolutionary scenarios discussed for low-mass binary X-ray sources in § Va could apply to them.

Using the results of our statistical analysis, we can discount the possibility of a dominant contribution of capture binaries to the integrated luminosity of early spirals. If this were the case, we would expect the integrated X-ray luminosity to follow a functional relationship of the form $l_X \propto l_B^\alpha$, with $\alpha \approx \frac{1}{4}$ (see Trinchieri and Fabbiano 1985), in contradiction to the observed linear dependence. Given the spread in the correlations, however, a fraction of the X-ray emission of early-type spirals could still originate from capture binaries in the inner bulge, as suggested by the observations of M31.

c) *The Production of Cosmic Rays and the Origin of the Radio Emission of Spiral and Irregular Galaxies*

Our analysis of the *Einstein* spiral and irregular sample shows that the correlation between radio continuum and X-ray luminosity is stronger than any of the relationships between the radio luminosity and the other variables under consideration.

The radio continuum emission of spiral galaxies at 1400 MHz is dominated by the nonthermal synchrotron emission of cosmic ray electrons interacting with the galactic magnetic fields (see, e.g., Ekers 1980). The X-ray emission, as discussed earlier, is likely to be dominated by binary X-ray sources. There is no obvious direct reason why these binaries should be in any way connected with the galactic magnetic fields. The relationship between nonthermal radio continuum and X-ray emission of spiral galaxies therefore points to a close connection between X-ray sources and cosmic ray production in spiral galaxies. Because of the relatively short cosmic ray lifetimes ($\tau \approx 2 \times 10^7$ yr, see Axford 1980 and references therein), it is not simple to account for this result in the widely accepted picture that links cosmic ray production with Type II supernovae (Lequex 1971). In systems with recent extensive star formation activity, like the LMC or the peculiar galaxies in Fabbiano, Feigelson, and Zamorani (1982), the same supernova explosions can be responsible for the cosmic ray production and the X-ray emission, both directly as supernova remnant X-ray sources or through the production of high-mass binary X-ray systems (the elapsed time after the supernova explosion for these systems to enter the X-ray emitting phase is $\sim 4 \times 10^6$ yr, see, e.g., van den Heuvel 1980). However, this cannot be the case in normal spiral galaxies, even if we restrict ourselves to Sbc and later types. In these galaxies a considerable portion of the X-ray emission ($\geq \frac{1}{2}$) originates from the older disk population (low-mass binaries), as we have discussed above. If these X-ray sources originate from binary systems composed of a massive and a low-mass star or from disrupted globular clusters, their evolution time to reach the X-ray emitting stage would be a few times 10^9 yr (see Webbink,

Rappaport, and Savonije 1983; Grindlay 1984). This is much longer than the cosmic ray lifetime in the disk of the galaxy ($\sim 2 \times 10^7$ yr, Axford 1980), making a direct link between cosmic ray production and X-ray source production impossible. In the alternative evolutionary scenarios of core collapse in an accreting white dwarf discussed in § Va, there is no such time constraint, since the onset of the X-ray phase could happen in a short time after the collapse. If the collapse involves a Type I supernova event (Canal, Isern, and Labay 1984), a large fraction ($\gtrsim \frac{1}{2}$) of the cosmic rays in spiral galaxies could originate in Type I supernovae. The connection between X-ray and radio emission could be an evolutionary link involving both Type I and Type II supernova events.

A more direct connection is, however, possible: binary X-ray sources could be the primary producers of cosmic ray electrons. Strong indications in favor of this hypothesis are given by the radio and X-ray observations of relativistic jets emerging from SS 433 and interacting with the surrounding medium (Hjellming and Johnston 1981; Watson *et al.* 1983). SS 433 is a massive X-ray binary in the Milky Way (Grindlay *et al.* 1984). Evidence of nuclear reactions that might be associated with the jets of SS 433 has also been reported (Lamb *et al.* 1983). Radio observations of Sco X-1, a low-mass binary X-ray source, also reveal the presence of a jet (Geldzahler *et al.* 1981). Gamma-ray observations of Her X-1 (Dowthwaite *et al.* 1984), Cyg X-3 (Samorski and Stamm 1983), and Vel X-1 (Protheroe, Clay, and Gerhardy 1984) also strongly suggest that these X-ray sources are sources of beamed cosmic ray particles (Vestrand and Eichler 1982).

Theoretically, the presence of beams of charged particles in binary X-ray sources could be accounted for by the presence of a central compact object and of a surrounding accretion disk, in analogy with beam models for active galactic nuclei (e.g., Rees 1980). As stated by Rees (1980), the creation of $e^+ - e^-$ pairs "is unavoidable in a compact region containing high energy particles, emitting X-rays and gamma-rays." The accretion disk would be responsible for the beaming. Kundt (1984) has explored the production of beams of electrons and positrons as a result of the interaction of the accreting matter with the magnetosphere of the compact star in a binary X-ray source.

From the point of view of energy balance, it could be possible for X-ray sources to account for most of the cosmic ray density in galaxies. The total cosmic ray source power is $\sim 3 \times 10^{40}$ ergs s^{-1} in the Milky Way (e.g., Axford 1980), within a factor of 10 of the total Galactic X-ray emission. Observations of SS 433 show that the power in the beams of this source could range between $\sim 10^{37}$ and $\sim 10^{41}$ ergs s^{-1} (Watson *et al.* 1983, and references therein), possibly orders of magnitude above the observed X-ray luminosity. The X-ray (2 keV)-to-radio (5 GHz) monochromatic flux ratios of two X-ray binaries, SS 433 and Cyg X-3, are $\sim 10^{-6}$ to 10^{-5} (using radio fluxes from Seaquist *et al.* 1982 and Molnar, Reid, and Grindlay 1984, and X-ray fluxes from the 4U catalog, Forman *et al.* 1978). These ratios are compatible with the nuclear X-ray (2 keV)-to-radio (5 GHz) monochromatic flux ratios of 3CR double-lobed radio galaxies (Fabbiano *et al.* 1984). Similar flux ratios for other low-mass X-ray binaries instead range from ~ 1 for Sco X-1 to ~ 100 for other "bulge"-type sources (Seaquist and Grindlay 1985). Some low-mass X-ray binaries must therefore be very inefficient radio sources, if they are to power the cosmic rays.

Our results indicate that either X-ray sources are the main

producers of cosmic rays, or X-ray source production is linked with cosmic ray production through Type I and II supernovae. In either case, the controversy over the nature of the radio emission of spiral galaxies can be finally resolved. Lequeux (1971) first suggested that the radio emission of spiral galaxies is due to the young Population I component, with Type II supernovae being the cosmic ray producers. This was followed by a considerable amount of debate, originated by different observational results. Some of these, like the excess radio emission observed in blue starburst galaxies (Biermann 1976), or the correlation between radio luminosity and blue colors or H α emission (Klein 1982; Kennicutt 1983), pointed to the young Population I as responsible for the radio emission. The smooth appearance of the radio disk emission and the lack of strong correlation with the spiral arm pattern, together with a correlation between radio and optical luminosity (Van der Kruit, Allen, and Rots 1979; Hummel 1981), suggested that the old disk Population I (age greater than 10^8 yr) was responsible for the radio emission. The main problem with the latter hypothesis was in finding a suitable class of objects in the old disk population that could be responsible for the production of cosmic rays. More recent work (e.g., Klein, Wielebinski, and Beck 1984, and references therein) invokes galactic magnetic fields as a mechanism for redistributing the cosmic rays produced by the young arm Population I to the whole galactic disk.

Our results suggest that the radio emission of spiral galaxies is both linked to the very young Population I component (as shown by the results on blue peculiar galaxies, see Fabbiano, Feigelson, and Zamorani 1982), and to the older Population I disk component. Type II supernovae or massive X-ray binary sources or both in the first case and Type I supernovae or low-mass X-ray binaries or both in the second would be responsible for the production of cosmic rays.

d) The Galactic Magnetic Fields

The nonthermal radio continuum emission of spiral galaxies is a function both of the density of cosmic rays and of the galactic magnetic field. We will discuss here the implications of our results for the properties of the magnetic fields of spiral galaxies.

The functional relationship between the radio continuum luminosity l_R , the cosmic ray density n_{cr} , and the magnetic field B is of the form $l_R \propto n_{cr} B^{1.73}$ (e.g., Ekers 1980). The exponent of B derives from the observed spectral shape of the radio continuum emission of spiral galaxies (Gioia, Gregorini, and Klein 1982). We have found a relationship of the form $l_X \propto l_R^\alpha$ between the X-ray and radio continuum luminosity of late-type spiral galaxies with $\alpha \approx 0.3-0.6$ (§ IIIc). Using this relationship, we derive that $l_X \propto (n_{cr} B^{1.73})^\alpha$. If the cosmic ray density is proportional to l_X (see § Vb), we then have that $B \propto l_X^\beta \propto l_R^{\beta\alpha}$, with $\beta \approx 1.3-0.4$. The flat functional relationship between l_X and l_R could then indicate that larger and brighter spiral galaxies have larger magnetic fields (see also Fabbiano, Trinchieri, and Macdonald 1984).

Using the above relationship and assuming again proportionality between l_X and n_{cr} , we obtain the result that the magnetic field of disk galaxies is a function of the cosmic ray density: $B \propto n_{cr}^\beta$, again with $\beta \approx 1.3-0.4$. This is in agreement with the conclusions of Parker (1971) that cosmic rays are responsible for the turbulent motions that generate the poloidal magnetic field. The effect of the nonuniform rotation on this field would then generate the azimuthal magnetic field.

The large bulges of early-type spirals are also likely to contain low-mass binary systems, whatever their evolutionary history (see above). If low-mass binaries in the disk do produce cosmic rays, these sources should also. Our data, however, suggest a lack of radio emission from the bulges of early spirals ($0 \leq T \leq 4$), pointing to an absence of strong ordered magnetic fields in the bulges. Supporting evidence comes from radio observations of normal elliptical galaxies (Hummel, Kotanyi, and Ekers 1983). These galaxies, which are similar systems to the spiral bulges (Faber 1981), are also fainter radio sources than spiral galaxies. This is consistent with the observational result (also in Faber 1981) that ellipticals and bulges of spirals rotate much less than the disks. The lack of rotation would impair the dynamo process (Parker 1971).

VI. CONCLUSIONS

Our statistical analysis of the spiral and irregular *Einstein* normal galaxy sample (LVS) has led to the following conclusions.

a) The X-ray luminosity is not directly correlated with the mass of the galaxies (as represented by the *H*-band luminosity or the *B-H* color). It is instead strongly correlated with the blue luminosity. This suggests that most X-ray sources, including the low-mass binaries (which in our Milky Way have traditionally been called "bulge" sources), are binary systems belonging both to the old disk Population I and the young arm Population I component.

b) There exists a real bulge population of X-ray sources that can contribute significantly to the X-ray luminosity of early-type spirals. Although a good fraction of these sources in the inner part of the bulge could be "capture" binaries (van den Heuvel 1980), others (like those in the outer bulge regions of

M31) cannot be similarly explained. The functional relationships between l_x and the blue and *H*-band luminosities are not consistent with capture binaries contributing to most of the X-ray emission of early-type spiral bulges.

c) X-ray sources (and low-mass X-ray binaries in particular) are closely related to the cosmic ray production in spiral galaxies. This could either be an evolutionary link, involving a supernova stage (both Type I and Type II) in the formation of binary X-ray sources, or X-ray binaries might themselves be the main producers of cosmic rays. The presence of radio jets in low-mass binaries, such as Sco X-1, and massive X-ray binaries, such as SS 433, and of γ -ray emission in the X-ray binaries Her X-1, Cyg X-3, and Vel X-1 supports this suggestion. The radio continuum emission of spiral galaxies would then originate from both the old disk Population I and the younger Population I component of the spiral arms.

d) Galactic magnetic fields are a function of the galaxy luminosity: larger and brighter spiral galaxies would have larger magnetic fields. The magnetic fields are also a function of the cosmic ray density, in agreement with the conclusions of Parker (1971) that cosmic rays are responsible for the turbulent motions that generate the poloidal magnetic field in the Galaxy. Our data also suggest a lack of radio emission from the bulges of early-type spirals. This would imply an absence of strong ordered magnetic fields in the bulges.

We wish to thank G. Zamorani for many interesting discussions on the subject of this paper and for suggestions on statistical techniques, J. Schmitt for the use of his statistical software, and J. Grindlay and J. Stocke for useful comments. We are indebted to M. Elvis for many discussions and critical readings of the manuscript. This work was supported under NASA contract NAS8-30751.

REFERENCES

- Aaronson, M. 1977, Ph.D. thesis, Harvard University.
 Aaronson, M., Huchra, J., and Mould, J. 1979, *Ap. J.*, **229**, 1.
 Aaronson, M., et al. 1982, *Ap. J. Suppl.*, **50**, 241.
 Aaronson, M., Mould, J., and Huchra, J. 1980, *Ap. J.*, **237**, 655.
 Avni, Y., Soltan, A., Tananbaum, H., and Zamorani, G. 1980, *Ap. J.*, **238**, 800.
 Axford, W. I. 1980, in *IAU Symposium 94, Origin of Cosmic Rays*, ed. G. Setti, G. Spada, and A. W. Wolfendale (Dordrecht: Reidel), p. 339.
 Biermann, P. 1976, *Astr. Ap.*, **53**, 295.
 Canal, R., Isern, J., and Labay, J. 1982, *Nature*, **296**, 225.
 ———. 1984, *Proc. Conf. on X-Ray Astronomy 1984* (Bologna), in press.
 de Vaucouleurs, G., de Vaucouleurs, A., and Corwin, H. G. 1976, *Second Reference Catalogue of Bright Galaxies* (Austin: University of Texas Press).
 Douthwaite, J. C., Harrison, A. B., Kirkman, I. W., Macrae, H. J., Orford, K. J., Turver, K. E., and Walmsley, M. 1984, *Nature*, **309**, 691.
 Dressel, L. L., and Condon, J. J. 1978, *Ap. J. Suppl.*, **36**, 53.
 Ekers, R. D. 1980, in *The Structure and Evolution of Normal Galaxies*, ed. S. M. Fall and D. Lynden-Bell (Cambridge: Cambridge University Press), p. 169.
 Elvis, M., and Van Speybroeck, L. 1982, *Ap. J. (Letters)*, **257**, L51.
 Fabbiano, G., Feigelson, E., and Zamorani, G. 1982, *Ap. J.*, **256**, 397.
 Fabbiano, G., Miller, L., Trinchieri, G., Longair, M., and Elvis, M. 1984, *Ap. J.*, **277**, 115.
 Fabbiano, G., and Trinchieri, G. 1984, *Ap. J.*, **286**, 491.
 Fabbiano, G., Trinchieri, G., and Macdonald, A. 1984, *Ap. J.*, **284**, 65.
 Faber, S. 1981, in *Astrophysical Cosmology: Proceedings of the Vatican Study Week on Cosmology and Fundamental Physics*, ed. H. A. Brück, G. V. Coyne, and M. S. Longair (Rome: Specola Vatican), p. 191.
 Fabian, A. C. 1981, in *The Structure and Evolution of Normal Galaxies*, ed. S. M. Fall and D. Lynden-Bell (Cambridge: Cambridge University Press), p. 181.
 Forman, W., Jones, C., Cominsky, L., Julien, P., Murray, S., Peters, G., Tananbaum, H., and Giacconi, R. 1978, *Ap. J. Suppl.*, **38**, 357.
 Geldzahler, B. J., Fomalont, E. B., Hilldrup, K., and Corey, B. E. 1981, *A. J.*, **86**, 1036.
 Giacconi, R. 1974, in *X-Ray Astronomy*, R. Giacconi and H. Gursky (Dordrecht: Reidel), p. 155.
 Giacconi, R., et al. 1979, *Ap. J.*, **230**, 540.
 Gioia, I. M., Gregorini, L., and Klein, U. 1982, *Astr. Ap.*, **116**, 164.
 Grindlay, J. E. 1984, *Adv. Space Res.*, Vol. 3, No. 10–12, p. 19.
 Grindlay, J. E., Band, D., Seward, F., Leahy, D., Weisskopf, M. C., and Marshall, F. E. 1984, *Ap. J.*, **277**, 286.
 Gursky, H. 1976, in *IAU Symposium 73, The Structure and Evolution of Close Binary Systems*, ed. P. Eggleton, S. Mitton, and J. Whelan (Dordrecht: Reidel), p. 19.
 Harnett, J. I. 1982, *Australian J. Phys.*, **35**, 321.
 Hjellming, M., and Johnston, K. L. 1981, *Ap. J. (Letters)*, **246**, L141.
 Hodge, P. 1983, *Pub. A.S.P.*, **95**, 721.
 Hummel, E. 1980, *Astr. Ap. Suppl.*, **41**, 151.
 ———. 1981, *Astr. Ap.*, **93**, 93.
 Hummel, E., Kotanyi, C. G., and Ekers, R. D. 1983, *Astr. Ap.*, **127**, 205.
 Jensen, E. B., Talbot, R. J., and Dufour, R. J. 1981, *Ap. J.*, **243**, 716.
 Kendall, M., and Stuart, A. 1976, *Advanced Theory of Statistics*, Vol. 2 (3d ed.; London: Griffin).
 Kennicutt, R. C. 1983, *Astr. Ap.*, **120**, 219.
 Kent, S. 1984, in preparation.
 Klein, U. 1982, *Astr. Ap.*, **116**, 175.
 Klein, U., Wielebinski, R., and Beck, R. 1984, *Astr. Ap.*, **135**, 213.
 Kundt, W. 1984, *Proc. July 1984 COSPAR Meeting* (Graz) (Elmsford, NY: Pergamon), in press.
 Lamb, R. C., Long, J. C., Mahoney, W. A., Riegler, G. R., Wheaton, W. A., and Jacobson, A. S. 1983, *Nature*, **505**, 57.
 Lequeux, J. 1971, *Astr. Ap.*, **15**, 42.
 Lightman, A. P., and Grindlay, J. E. 1982, *Ap. J.*, **262**, 145.
 Long, K. S., D'Odorico, S., Charles, P. A., and Dopita, M. A. 1981, *Ap. J. (Letters)*, **246**, L61.
 Long, K. S., Helfand, D. S., and Grabelsky, D. A. 1981, *Ap. J.*, **248**, 925.
 Long, K. S., and Van Speybroeck, L. P. 1983, in *Accretion Driven X-Ray Sources*, ed. W. Levin and E. P. J. Van den Heuvel (Cambridge: Cambridge University Press), p. 41 (LVS).
 Molnar, L. A., Reid, M. J., and Grindlay, J. E. 1984, *Nature*, **310**, 662.
 Nomoto, K. 1984, in *Problems of Collapse and Numerical Relativity*, ed. D. Bancel and M. Signore (Dordrecht: Reidel), p. 89.
 Nulsen, P. E. J., Stewart, G. C., and Fabian, A. C. 1984, *M.N.R.A.S.*, **208**, 185.
 Palumbo, G. G. C., Fabbiano, G., Fransson, C., and Trinchieri, G. 1985, *Ap. J.*, submitted.

- Parker, E. N. 1971, *Ap. J.*, **168**, 239.
- Protheroe, R. J., Clay, R. W., and Gerhardy, P. R. 1984, *Ap. J. (Letters)*, **280**, L47.
- Rappaport, S., Joss, P. C., and Webbink, R. F. 1982, *Ap. J.*, **254**, 616.
- Rees, M. J. 1980, in *IAU Symposium 94, Origin of Cosmic Rays*, ed. G. Setti, G. Spada, and A. W. Wolfendale (Dordrecht: Reidel), p. 139.
- Rubin, V. C., Ford, W. K., Jr., Thonnard, N., and Burstein, D. 1982, *Ap. J.*, **261**, 439.
- Samorski, M., and Stamm, W. 1983, *Ap. J. (Letters)*, **268**, L17.
- Sandage, A., and Tammann, G. A. 1981, *A Revised Shapley-Ames Catalog of Bright Galaxies* (Washington: Carnegie Institution Pub. 635).
- Schmitt, J. H. M. 1985, *Ap. J.*, **293**, 178.
- Sequist, E. R., Gilmore, W. S., Johnston, K. J., and Grindlay, J. E. 1982, *Ap. J.*, **260**, 220.
- Sequist, E. R., and Grindlay, J. E. 1985, in preparation.
- Seward, F. D., and Mitchell, M. 1980, *Ap. J.*, **243**, 736.
- Simien, F., and de Vaucouleurs, G. 1983, *IAU Symposium 100, Internal Kinematics and Dynamics of Galaxies*, ed. E. Athanassoula (Dordrecht: Reidel), p. 375.
- Stanger, V., and Schwarz, J. 1984, preprint.
- Tananbaum, H., and Tucker, W. H. 1974, in *X-Ray Astronomy*, R. Giacconi and H. Gursky (Dordrecht: Reidel), p. 207.
- Tananbaum, H., Wardle, J. F. C., Zamorani, G., and Avni, Y. 1983, *Ap. J.*, **268**, 60.
- Trinchieri, G., and Fabbiano, G. 1985, *Ap. J.*, **296**, 447.
- Trinchieri, G., Fabbiano, G., and Palumbo, G. G. C. 1985, *Ap. J.*, **290**, 96.
- Tully, R. B., and Fisher, J. R. 1977, *Astr. Ap.*, **54**, 661.
- Tully, R. B., Mould, J. R., and Aaronson, M. 1982, *Ap. J.*, **257**, 527.
- van den Heuvel, E. P. J. 1980, in *X-ray Astronomy, Proc. NATO Advanced Study Institute held at Erice, Sicily, July 1-14, 1979*, ed. R. Giacconi and G. Setti (Dordrecht: Reidel), p. 119.
- Van der Kruit, P. C., Allen, R. J., and Rots, A. H. 1977, *Astr. Ap.*, **55**, 421.
- Van Speybroeck, L., Epstein, A., Forman, W., Giacconi, R., Jones, C., Liller, W., and Smarr, L. 1979, *Ap. J. (Letters)*, **234**, L45.
- Vestrand, W. T., and Eichler, D. 1982, *Ap. J.*, **261**, 251.
- Watson, M. G., Willingale, R., Grindlay, J. E., and Seward, F. D. 1983, *Ap. J.*, **273**, 688.
- Watson, M. G., Stranger, V., and Griffiths, R. E. 1984, *Ap. J.*, **286**, 144.
- Webbink, R. F., Rappaport, S., and Savonije, G. J. 1983, *Ap. J.*, **270**, 678.
- White, R. E., III, and Chevalier, R. A. 1984, *Ap. J.*, **280**, 561.
- Whitmore, B. C. 1984, *Ap. J.*, **278**, 61.

G. FABBIANO and G. TRINCHIERI: High Energy Astrophysics Division, Center for Astrophysics, 60 Garden Street, Cambridge, MA 02138

A STATISTICAL ANALYSIS OF THE *EINSTEIN* NORMAL GALAXY SAMPLE. II. ELLIPTICAL AND S0 GALAXIES

G. TRINCHIERI AND G. FABBIANO

Harvard-Smithsonian Center for Astrophysics

Received 1984 November 13; accepted 1985 March 18

ABSTRACT

The statistical analysis of a sample of 29 elliptical and S0 field galaxies observed with the *Einstein* observatory is presented. The data show a correlation between the X-ray and the optical blue luminosity of the form $L_x \propto l_B^{1.64 \pm 0.15}$. This is significantly steeper than the correlation observed in spiral and irregular galaxies: $L_x \propto l_B^{1.08 \pm 0.07}$.

Several mechanisms for the origin of the X-ray emission in these galaxies have been investigated to explain the observed correlation. Most likely two separate mechanisms are present: thermal radiation from hot gas is required to explain the high-luminosity massive objects ($M \gtrsim 5 \times 10^{11} M_\odot$, $L_x \gtrsim 10^{41}$ ergs s⁻¹), while a collection of low-mass binary sources can explain the low-luminosity, low-mass objects.

A comparison between radio-loud and radio-quiet galaxies shows that high optical luminosity, or high mass, is required for the onset of nuclear activity, at both radio and X-ray wavelengths. However, this is not sufficient to ensure the presence of active nuclear sources, and a second parameter (at least) is needed.

A comparison between radio-loud elliptical galaxies and QSOs shows that the same X-ray emission mechanism that is operating in QSOs could explain the high X-ray luminosity end of the radio-loud galaxy distribution.

Subject headings: galaxies: nuclei — galaxies: stellar content — galaxies: X-rays

I. INTRODUCTION

In the companion paper (Fabbiano and Trinchieri 1985, hereafter FT) we discuss the X-ray properties of spiral and irregular galaxies and find that their X-ray emission is dominated by the integrated output of binary X-ray sources, mostly belonging to the Population I component.

A different picture of the nature of the X-ray emission of elliptical and S0 galaxies is given by the results of the X-ray observations published so far. Extended thermal emission has been associated with elliptical galaxies in the Virgo Cluster (e.g., M87, Fabricant and Gorenstein 1983; M84 and M86, Forman, Jones, and Tucker 1984), in poor groups (e.g., NGC 5848, Biermann and Kronberg 1983) and in more isolated galaxies (Nulsen, Stewart, and Fabian 1984). However, high-resolution observations of the bulge of M31 (Van Speybroeck *et al.* 1979) reveal that the X-ray emission of this spheroidal system is composed of many bright pointlike sources. The results of FT also suggest that all early-type spiral galaxies have similar bulge components in their X-ray emission. Bulges are believed to be spheroidal systems very similar to elliptical galaxies (e.g., Faber 1981).

Establishing the presence of hot X-ray emitting gas or X-ray emitting stellar remnants or both in elliptical galaxies will be crucial for a more complete understanding of these stellar systems. The content of elliptical and S0 galaxies, both in the form of visible matter (stars) and of gas, has been a subject of debate and study for many years. Elliptical galaxies are generally believed to contain predominantly an old, metal-rich stellar population dominated by K and M giants (see Frogel *et al.* 1975*a, b*; Gunn, Stryker, and Tinsley 1981). Models for continuous star formation predict colors in general agreement with the observed integrated colors, but they also predict a color gradient from red to blue toward the nucleus, contrary to what is generally observed (Larson and Tinsley 1974; Faber

1973). This suggests that either the star formation occurs with a very steep or truncated initial mass function (IMF), or the star formation occurs in bursts (see Faber and Gallagher 1976; Sanders 1981).

Interstellar gas, either ionized or neutral, has been searched for in elliptical galaxies. About 10^9 – $10^{10} M_\odot$ of interstellar gas should reside in these galaxies as a result of stellar evolution (see Faber and Gallagher 1976, and references therein). Since observations in H I and at optical wavelengths have mostly failed to detect cold or ionized gas in elliptical and S0 galaxies, Faber and Gallagher (1976) suggested hot galactic winds as a gas removal mechanism, although they acknowledged that star formation resulting only in low-mass stars could be a suitable alternative. Hot gas in isolated elliptical galaxies might be directly detectable in X-rays, as it has been detected in M87 and other Virgo Cluster galaxies (see above).

The X-ray observations might also provide a new insight into the problem of nuclear activity in early-type galaxies. The limited observational evidence to date points toward mass and ellipticity (Heckman 1983; Heeschen 1970; Hummel, Kotanyi, and Ekers 1983) as crucial parameters for the onset of nuclear activity. These parameters might regulate the flow of gas accreting to the cores and feeding a central black hole. X-ray observations of a sample of normal elliptical galaxies of different optical luminosity (and mass) could help in pinpointing the critical mass for gas retention and onset of activity.

In this paper we study the statistical properties of the X-ray emission from a sample of 29 relatively isolated, normal elliptical and S0 galaxies. The results will be compared with those obtained for a sample of normal spiral and irregular galaxies (Fabbiano, Trinchieri, and Macdonald 1984; FT) to investigate the origin of the X-ray emission in early-type galaxies and the possible emission mechanisms. The influence of a powerful radio source and the onset of nuclear activity will also be

investigated by comparing our normal sample with the 3CR galaxies sample (Fabbiano *et al.* 1984).

II. THE SAMPLE

Most of the galaxies used in the following analysis are part of a sample of normal galaxies compiled by Long and Van Speybroeck (1983, hereafter LVS) from the data of several observers. Four additional galaxies discussed by Nulsen, Stewart, and Fabian (1984), NGC 1172, NGC 1395, NGC 2974, and NGC 6876, have been included. The resulting sample consists of 29 early-type galaxies (with morphological parameter $T < 0$ as defined by de Vaucouleurs, de Vaucouleurs, and Corwin 1976) that were observed in X-rays with the *Einstein* observatory. The X-ray luminosities in the 0.5–3.0 keV band and the distances of all the galaxies are taken from LVS and Nulsen, Stewart, and Fabian (1984). The X-ray luminosity of NGC 4636 given in LVS might be underestimated by a factor of ~ 1.5 (see Stanger and Schwarz 1984). Since the data in LVS were analyzed in a uniform way, and we do not have a second estimate of the X-ray luminosity of most of the galaxies, we have chosen to use the LVS X-ray luminosities for all galaxies. Using the more recent estimate of the luminosity of NGC 4636 would not change our conclusions.

Blue magnitudes and color indices $U - B$ and $B - V$ are from de Vaucouleurs, de Vaucouleurs, and Corwin (1976). We have used the corrected face-on total magnitude and colors when available. Corrected infrared H (1.6 μm) magnitudes are available for 17 galaxies (Persson, Frogel, and Aaronson 1979; Aaronson 1977), and the radio continuum fluxes, or upper limits, at 1400 MHz, for 18 galaxies (Hummel 1980). The fluxes at 408 MHz (Harnett 1982) and 2380 MHz (Dressel and Condon 1978) are available for four additional galaxies. For consistency with FT, we have used monochromatic values for the fluxes (mJy) and luminosities ($\text{ergs s}^{-1} \text{Hz}^{-1}$). The 2 keV X-ray monochromatic luminosities are derived from the 0.5–3.0 keV band luminosities. In Table 1 we list the galaxies in this sample, together with their infrared (H), optical (B), and X-ray (2 keV) monochromatic luminosities.

Due to the selection criteria, the resulting sample is not statistically complete. However, we believe it is a representative sample of normal nearby early-type galaxies. Figure 1 shows the distribution of blue apparent magnitude m_B and absolute magnitude M_B for the 29 galaxies used in this work. They cover a wide absolute magnitude range between $M_B \approx -18$ and $M_B \approx -23$ with colors in the range of normal elliptical and S0 colors (Larson and Tinsley 1978; see Fig. 9a in LVS). With the exception of NGC 1316 (Fornax A) and NGC 5532 (3C 296), they have weak or undetected radio continuum emission and do not show strong nuclear activity. They can also be regarded as a sample of relatively isolated galaxies. They are not at the center of rich clusters, although some are in poor groups (e.g., NGC 6876 in Pavo) or at the outskirts of the Virgo Cluster (e.g., NGC 4636 or NGC 4649).

III. RESULTS

Our analysis of the sample of elliptical and S0 galaxies is similar to our analysis of the sample of spiral and irregular galaxies (for details on the analysis, see FT).

a) The Distribution of X-Ray Luminosities and X-Ray-to-Optical Flux Ratios

Figure 2a shows the distribution of 0.5–3.0 keV X-ray luminosities for the 19 galaxies in the sample. Nineteen galaxies

TABLE 1
MONOCHROMATIC LUMINOSITIES
($\text{ergs s}^{-1} \text{Hz}^{-1}$)

NGC	D (Mpc)	$\log l_H$	$\log l_B$	$\log l_x$
524.....	51.90	...	29.66	23.18
720.....	38.58	...	29.54	23.27
936.....	26.64	29.79	29.27	<22.91
1172.....	30.00	...	28.63	<22.12
1316.....	32.64	30.54	30.00	23.59
1332.....	30.40	29.91	29.36	22.89
1380.....	29.28	29.91	29.36	22.75
1395.....	34.00	29.94	29.31	23.01
1533.....	11.20	...	28.20	21.46
1574.....	19.98	29.38	28.93	<22.51
2859.....	29.26	...	29.11	<22.41
2974.....	40.00	29.86	29.34	22.85
3377.....	15.98	28.20	28.80	<21.89
3489.....	15.98	...	28.81	<22.01
3585.....	24.74	29.73	29.26	22.05
3818.....	31.66	...	28.75	<22.69
3923.....	32.70	29.94	29.46	22.98
4251.....	18.44	...	28.76	<21.76
4382.....	20.26	29.90	29.41	22.77
4459.....	20.78	29.50	28.94	<22.36
4636.....	25.44	29.85	29.42	23.19
4638.....	20.26	...	28.64	21.50
4649.....	21.86	30.04	29.56	23.50
4697.....	26.14	30.03	29.57	22.76
5102.....	7.90	28.60	28.54	<21.76
5532.....	142.12	...	29.98	23.85
5866.....	19.40	29.56	29.15	22.25
5898.....	42.56	...	29.15	22.62
6876.....	80.00	...	29.46	23.76

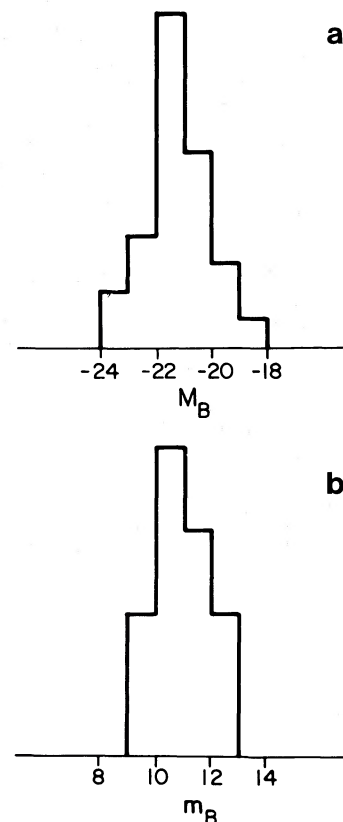


FIG. 1.—Distribution of (a) blue absolute magnitudes and (b) apparent magnitudes.

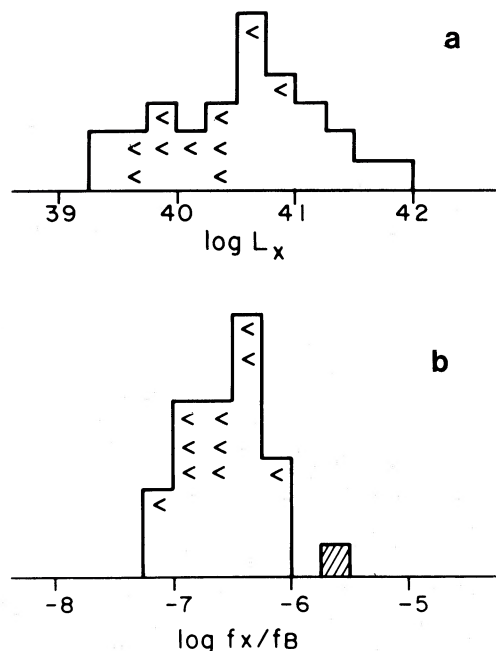


FIG. 2.—(a) Distribution of the X-ray luminosities L_x for the galaxies in the sample. (b) Distribution of the X-ray-to-optical flux ratios of f_x/f_B . The hatched box represents NGC 6876, for which only a Harvard magnitude is listed in de Vaucouleurs, de Vaucouleurs, and Corwin (1976).

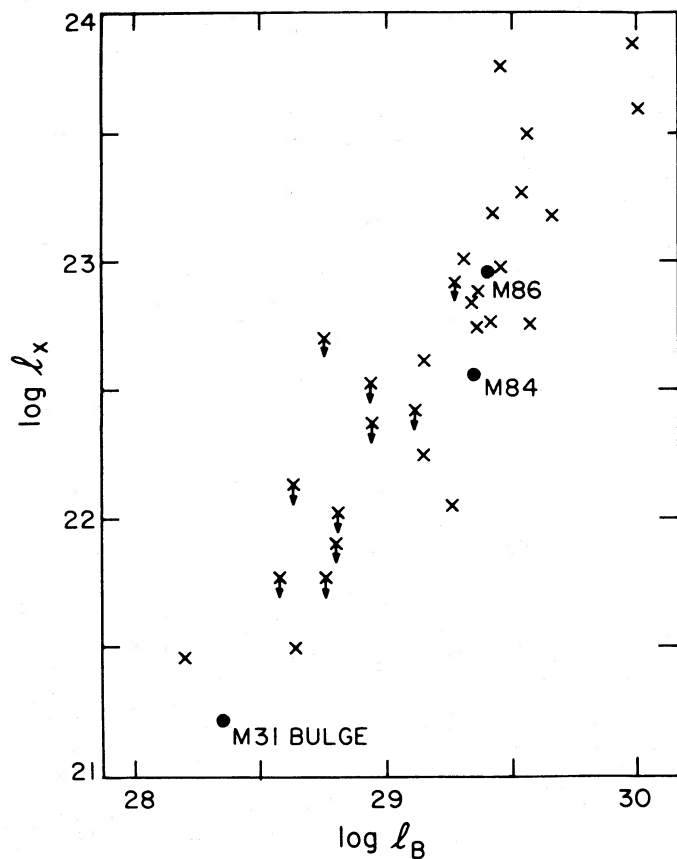


FIG. 3a

(~65%) were detected with X-ray luminosities in the range 2×10^{39} to 6×10^{41} ergs s^{-1} . The mean X-ray luminosity of the galaxies in the sample is $\langle L_x \rangle = 9 \times 10^{40}$ ergs s^{-1} , calculated using the “detection and bounds” (DB) method (Avni *et al.* 1980; Avni 1984; FT). As already noted by LVS, elliptical and S0 galaxies have on average a higher X-ray luminosity than spiral and irregular galaxies, although the two distributions overlap for more than a decade (see FT). The X-ray-to-optical monochromatic flux ratios f_x/f_B of early-type galaxies have a narrow distribution that ranges from 6×10^{-8} to 9×10^{-7} and is similar to the f_x/f_B distribution for late-type galaxies (FT), although less peaked (Fig. 2b).

b) Correlation Between X-Ray and Other Integrated Quantities

In Figure 3a the monochromatic X-ray luminosity l_x is plotted versus the optical blue luminosity l_B . The corresponding fluxes are plotted in Figure 3b. A correlation is evident in both cases. In order to give a quantitative estimate of the confidence level of each correlation, we applied the Spearman rank correlation test to our data, as in FT. The correlation coefficients r_{SR} and corresponding probabilities P_{SR} of a chance correlation are shown in Table 2. We calculated the correlation coefficients using the detections only (column A) and using both detections and bounds after assigning a worst case rank to the upper limits (column B). Since the latter coefficient represents a lower limit to the significance level of the correlation, we are confident that both the correlations found between the fluxes and the luminosities are real. The sample is not X-ray flux-limited, both detections and upper limits were included in the analysis, and there is a correlation also between the fluxes, so we can exclude the possibility that the correlation between the luminosities is due to a distance bias.

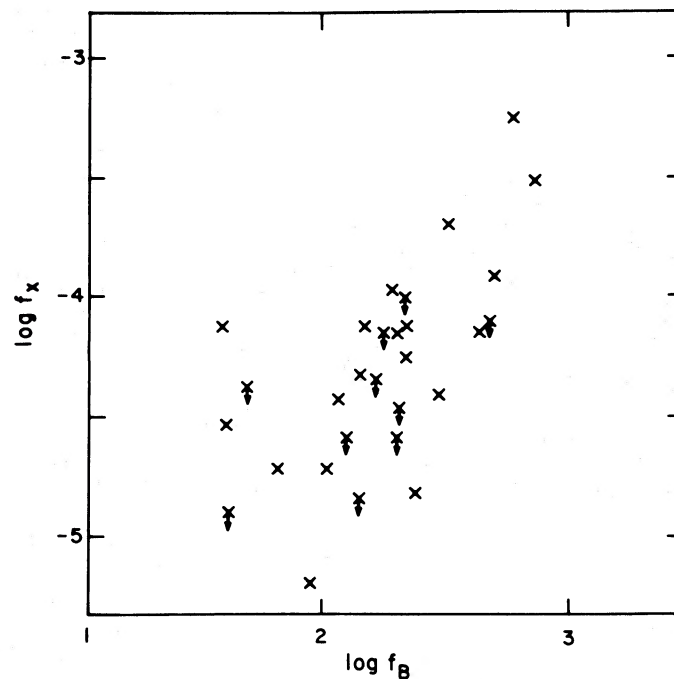


FIG. 3b

FIG. 3.—(a) Plot of the X-ray monochromatic 2 keV luminosity against the blue luminosity in units of ergs s^{-1} Hz^{-1} . M84, M86 and the bulge of M31 are also shown. (b) The X-ray monochromatic flux against blue flux in units of mJy.

TABLE 2
SPEARMAN RANK CORRELATION COEFFICIENTS AND PROBABILITIES
(one-tailed)

CORRELATIONS	A			B		
	N	r_{SR}	P_{SR}	N	r_{SR}	P_{SR}
l_x vs. l_B	19	0.82	$\sim 1 \times 10^{-5}$	29	0.79	$< 1 \times 10^{-6}$
f_x vs. f_B	19	0.66	$\sim 1 \times 10^{-3}$	29	0.32	$\sim 5\%$

NOTE.—A, detections only; B, "worst case" ranking for upper limits.

The blue magnitude is the only quantity for which information is available for all the galaxies. Twenty-six of the 29 galaxies have published $B-V$ colors from which we can derive the V magnitudes. Infrared H ($1.6 \mu\text{m}$) magnitudes have been published for about half the galaxies in the sample. To find the functional dependence of l_x on l_B , l_V , and l_H , we analyzed the data using the DB method (see FT). The method allows us to use the information given by both detections and upper limits in the X-ray data to derive the parameters that best describe the correlation. The assumptions to be made are that the dependence can be represented by a straight line, that the points are normally distributed around the best fit line with a spread σ , and that both detections and bounds are from the same parent population. The results are summarized in Table 3. In all instances the relation between X-ray and optical-infrared luminosities can be fitted with a power law with exponent $\alpha \approx 1.6$.

We also find that bluer early-type galaxies tend to have lower X-ray luminosities. However, we would expect this correlation as a consequence of the correlation between X-ray and optical luminosity and of the already established correlations between the optical magnitude and galaxy colors (see van den Bergh 1975, and references therein). Only about five galaxies of the present sample have radio continuum fluxes available in the literature. Therefore no useful information can be obtained on a possible correlation between X-ray and radio emission in early-type galaxies with the data available at present. This point will be addressed more fully in a future paper, using recently obtained radio flux measurements (Klein *et al.*, in preparation).

c) Comparison with Normal Spiral and Irregular Galaxies

Fabbiano, Trinchieri, and Macdonald (1984) and FT studied the statistical X-ray properties of spiral and irregular galaxies. They found that the X-ray luminosity of those galaxies is correlated with the optical luminosity with a functional dependence $l_x \propto l_B^{1.08 \pm 0.07}$.

TABLE 3
LINEAR FIT COEFFICIENTS AND DISPERSION

Y^a	X^a	A	99% Confidence Range	B	σ
$\log l_x$	$\log l_B$	1.64 ± 0.15	1.26–2.05	–25.4	0.30
$\log l_x$	$\log l_V$	1.52 ± 0.14	1.2 –1.86	–22.3	0.25
$\log l_x$	$\log l_H$	$1.65^{+0.25}_{-0.35}$	1.00–2.40	–26.5	0.25
$\log f_x$	$\log f_B$	$0.8^{+0.30}_{-0.29}$	0.20–1.50	–6.2	0.40
$\log f_x$	$\log f_V$	$1.1^{+0.29}_{-0.15}$	0.55–1.7	–7.2	0.35
$\log f_x$	$\log f_H$	1.55 ± 0.35	0.65–2.45	–8.7	0.30

^a $Y = AX + B$ with a dispersion σ around the straight line.

The elliptical and S0 galaxies show a correlation between l_x and l_B , with a much steeper functional dependence: $l_x \propto l_B^{1.64 \pm 0.15}$. The lower boundary of the 99% confidence region on the exponent, ~ 1.26 , is higher than the upper boundary of the 99% confidence region found for spiral galaxies, which is $\lesssim 1.23$. The probability that the slope obtained for the spiral and irregular galaxy sample could fit the early-type sample is $P \approx 10^{-4}$.

A clearer representation of this result is shown in Figure 4. Here we plot the distribution of the residuals obtained from the sample of early-type galaxies after removing the best fit obtained above (Fig. 4a). The residuals are normally distributed around a mean of zero. On the contrary, the residuals obtained for early-type galaxies about the best fit regression line of the spiral and irregular galaxy sample (FT) are systematically displaced towards negative values (Fig. 4b), contrary to what would be expected if the present samples could be fitted with the same parameters as the FT sample. We can quantify this difference by applying the Kolmogorov-Smirnov (KS) test to the distributions of residuals we obtained. Given the presence of bounds in the data, we could not apply the KS test directly. However, since we are testing whether the two distributions differ, we can estimate how the bounds should be distributed to make the two distributions more similar. This corresponds to having all the bounds in Figure 4b in the highest bin ($\geq +0.4$) and those in Figure 4a at their value. The KS test applied to the distributions thus obtained gives a probability of $\sim 5\%$ that the two distributions are alike. This should be regarded as a maximum value, since we have assumed the most unfavorable distribution of the bounds. Schmitt (1985) has adapted to the field of astronomy some statistical methods for the comparison of two samples in the presence of bounds in the data. We have applied the three tests in Schmitt, namely the logrank, Gehan, and Wilcoxon tests, to the two distributions of residuals in Figure 4. The results are consistent with the "adapted" KS test discussed above: we find a probability $P \approx 5\%$ for the logrank test and $P \lesssim 2\%$ for

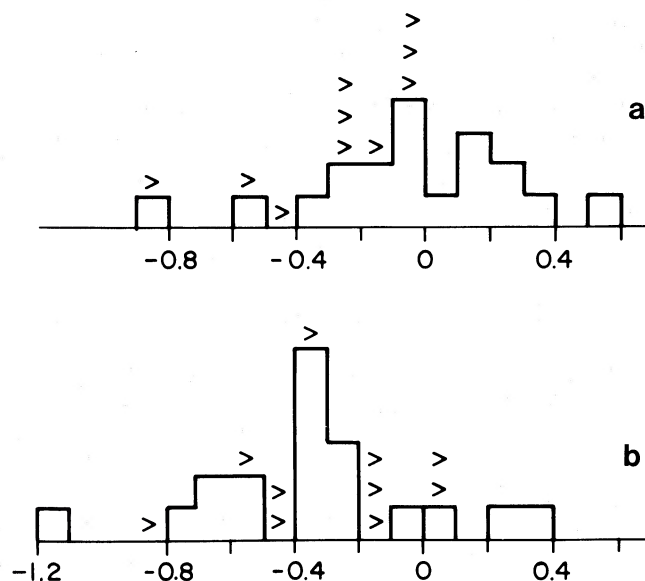


FIG. 4.—(a) Distribution of the residuals obtained for the elliptical and S0 galaxy sample after subtracting the best fit $\log l_x = 1.64 \log l_B - 25.4$. (b) Same, using $\log l_x = 1.08 l_B - 9.2$.

the Gehan and Wilcoxon tests that the two distributions are alike.

IV. DISCUSSION

In § III, we have shown that the X-ray luminosity of elliptical and S0 galaxies is correlated with their blue luminosity with a functional dependence of the form $l_x \propto l_B^{1.64 \pm 0.15}$. The same functional dependence is found between the X-ray luminosity and the infrared luminosity: $l_x \propto l_H^{1.65 \pm 0.30}$. This similarity is not surprising, since in these galaxies the infrared to optical color has a narrow distribution (Persson, Frogel, and Aaronson 1979). Since the correlation of l_x and l_H is derived using only about half the galaxies in the sample and does not introduce new information, we will not discuss it further. These correlations indicate that the origin of the X-ray emission in early-type galaxies is closely connected to the luminous mass of the galaxy. In particular, the X-ray luminosity is a steep function of the mass, i.e., the more massive galaxies have a higher X-ray luminosity per unit mass. This is different from the result found for spiral and irregular galaxies where, as shown in FT, the X-ray luminosity is a linear function of the blue luminosity ($l_x \propto l_B$), but not of the infrared luminosity ($l_x \propto l_H^{0.74}$), and there is evidence that star formation, rather than mass, is a fundamental parameter for the X-ray emission.

The steep dependence of the X-ray emission on the optical emission in elliptical and S0 galaxies suggests either a different origin for the X-ray emission than in spiral and irregular galaxies, or at least the presence of an additional X-ray emitting component. The X-ray observations of a few nearby galaxies, both isolated and in sparse regions of clusters, have shown that the X-ray emission has a scale comparable to or larger than the optical extent (Nulsen, Stewart, and Fabian 1984; Stanger and Schwarz 1984; Forman, Jones, and Tucker 1985). However, due to the combination of the limited sensitivity and angular resolution of the *Einstein* observatory with the distance and the relatively small angular size of elliptical galaxies, individual sources could not be resolved in those galaxies. M32, the dwarf elliptical companion of M31, is close enough for the IPC to detect individual binary sources. The observations suggest the presence of two sources coincident with the galaxy (see Van Speybroeck and Bechtold 1981).

In the discussion below we consider two plausible explanations for the X-ray emission from normal elliptical and S0 galaxies: the thermal radiation from a hot interstellar medium, and the integrated emission of individual sources. We also discuss the possibility of a contribution from a nuclear source and the onset of nuclear activity in early-type galaxies. In what follows, we have assumed a constant mass-to-light ratio M/L of 10. With this choice, we will be consistent with the work of White and Chevalier (1984; see below).

a) Gas

Bechtold *et al.* (1983) and Forman, Jones, and Tucker (1984) find extended X-ray emission associated with elliptical galaxies in clusters, which they interpret as thermal radiation from hot gaseous coronae. They suggest that this gas is expelled through the galactic winds and is confined near the galaxies by the pressure of the intergalactic medium. The galaxies M84 and M86 are plotted in Figure 3a as examples of hot gaseous coronae.

However, such phenomena are only expected in galaxies in clusters, where the external medium is dense enough to stop the wind and trap the hot gas around the galaxies. For isolated

galaxies, the estimated X-ray luminosities of the galactic winds would be too low to be detected (Mathews and Baker 1971). Two alternative mechanisms for the thermal emission of hot gas have been investigated. Forman, Jones, and Tucker (1985) suggest that hot coronae around galaxies could be a property of both cluster and isolated early-type galaxies. The gas would be bound to the galaxies by massive dark halos that extend beyond the optical image. Alternatively Nulsen, Stewart, and Fabian (1984); White and Chevalier (1984); and Stanger and Schwarz (1984) suggest a mechanism of infalling accreting gas similar to that observed in the centers of rich clusters of galaxies.

It is not the purpose of this paper to investigate in detail the mechanisms responsible for the thermal emission from hot gas, i.e., hot coronae or inflows. We can, however, compare the predictions of the models with the observations. The results can be seen in Figure 5. Neither model can explain the whole range of the observations and the relationship $l_x \propto l_B^{1.64}$. The hot coronae model predicts a functional dependence of the X-ray on the optical luminosity of the form $l_x \propto l_B^{2.0}$ (Forman, Jones, and Tucker 1985). Although in general agreement with the data, this is steeper than the best fit slope of 1.64 derived above. Moreover, this model would predict that even at low X-ray luminosities the X-ray emission is dominated by hot gas emission. This is in disagreement with the high-resolution X-ray observations of the bulge of M31, where pointlike sources clearly dominate the emission (Van Speybroeck *et al.* 1979).

Nulsen, Stewart, and Fabian (1984) suggested that, on the assumption of a steady cooling flow and no supernova energy input, $L_x \approx L_v^{1.5}$. This relationship would be in agreement with the correlation that we find. However, this phenomenon must fail at the low luminosities, because no gaseous component was found in the bulge of M31 (Van Speybroeck *et al.* 1979). The cooling flow calculations of White and Chevalier (1984), which include supernova energy input, instead show that the X-ray luminosity should be a roughly linear function of the mass, hence of the optical luminosity. This is in disagreement with the data, if the entire range of luminosities is considered. If the cooling flow model is applied to high-luminosity objects (see Nulsen, Stewart, and Fabian 1984; Stanger and Schwarz 1984), the results are in agreement with the observations. At lower luminosities, the White and Chevalier model predicts too much X-ray emission. To be consistent with the data, it would need to be truncated below an optical luminosity of few times 10^{29} ergs s⁻¹ Hz⁻¹.

b) Individual Sources

The observations of spiral galaxies have shown that binary sources make the major contribution to the X-ray emission in those galaxies. Although we do not have the same detailed information on elliptical and S0 galaxies, it is reasonable to assume that if discrete X-ray sources are responsible for the observed X-ray emission, these are probably associated with low-mass stars and low-mass binary systems, either in the main body of the galaxy or in globular clusters.

i) Low-Mass Stars

The stellar component contribution is probably only a fraction of the observed X-ray luminosity in elliptical and S0 galaxies. Feigelson *et al.* (1981) have estimated that the diffuse X-ray emission observed in Cen A can be accounted for by dM dwarfs only if their median X-ray luminosity is higher than

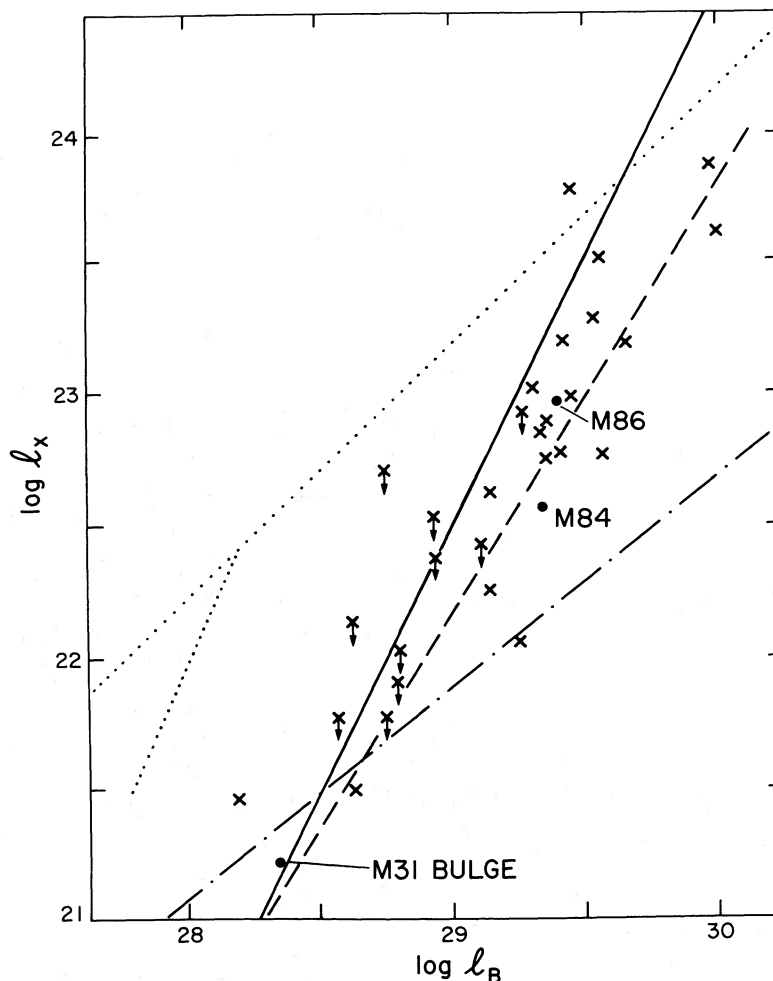


FIG. 5.—Same as Fig. 3a. The lines represent the different models considered: *dashed line*, best fit $l_x \propto l_B^{1.64}$; *solid line*, predicted dependence and normalization from the model of Forman, Jones, and Tucker (1985); *dot-dashed line*, individual sources; *dotted lines*, White and Chevalier (1984) model for $T \geq 1 \times 10^6$ K and $T \geq 2 \times 10^6$ K, in the assumption of supernova energy input.

that observed in M stars in the Milky Way. With similar arguments, we can estimate that the stellar component could contribute $\sim 1\%$ to 10% of the observed X-ray luminosity.

ii) Globular Cluster Sources

Both in our galaxy and in M31, $\sim 10\%$ of the known globular clusters have been detected in X-rays with $L_x > 10^{36}$ ergs s^{-1} (Hertz and Grindlay 1983; LVS). However, the average X-ray luminosity of globulars is higher in M31 (Van Speybroeck and Bechtold 1981). The galaxies in our sample should have on the average between ~ 500 and $\sim 10,000$ globular clusters if the number of globular clusters is a linear function of the optical luminosity (hence of the luminous mass, Harris and Racine 1979). If we assume that the distribution in X-ray luminosity for globular cluster X-ray sources in these galaxies is the same as in M31, we expect that these sources will contribute between $\sim 2 \times 10^{39}$ and $\sim 4 \times 10^{40}$ ergs s^{-1} to the total X-ray luminosity of early-type galaxies. This would represent a significant fraction of the X-ray luminosity for the lower mass objects ($M_T \lesssim 10^{11} M_\odot$) but only a few percent of the L_x for higher mass galaxies.

iii) Low-Mass Binary Sources

The detailed observations of the bulge of M31 in X-rays have shown that the emission is dominated by pointlike

sources with $L_x \gtrsim 10^{37}$ ergs s^{-1} (Van Speybroeck *et al.* 1979). As often discussed in the literature (e.g., Faber 1981, and references therein), bulges are indistinguishable from elliptical galaxies in their surface brightness profiles, broad-band colors, and velocity dispersions. This would suggest that the same pointlike sources that are observed to dominate the X-ray emission of the bulge of M31 are very likely to be present in elliptical and S0 galaxies as well. Figure 3a shows that the bulge of M31 lies on the correlation between l_x and l_B of elliptical and S0 galaxies, among the low-luminosity objects. The similarity between bulges and low-luminosity elliptical galaxies is thus likely to extend to their X-ray emission.

The high X-ray luminosity of the X-ray sources and the stellar population present in bulges indicate that most likely these sources are low-mass binary systems (see also Vader *et al.* 1982, and references therein). However, the X-ray observations of the bulge of M31 (see Van Speybroeck *et al.* 1979) suggest the presence of two different populations, the higher X-ray luminosity "inner bulge" sources clustering in the inner 400 pc and the lower L_x "outer bulge" sources.

Several mechanisms for the formalism of these sources have been suggested. A low-mass star may capture an evolved object. To provide the high X-ray luminosity of these sources, the captured object should be either a neutron star or a black

hole. Given the stellar density distribution, the capture mechanism could explain the inner bulge sources observed in M31 (see Van den Heuvel 1980), but fails to explain the formation of ("outer bulge") sources in less dense regions. Vader *et al.* (1982) argue against the formation of X-ray binaries by capture even in the innermost region of the bulge. They observe that since the binary X-ray sources and novae are similar systems, the capture mechanism should affect both similarly and result in a comparable distribution of X-ray sources and novae. The observed distribution of novae shows a "hole" in the center (Rosino 1973) not observed in the X-ray source distribution, which closely follows the light distribution. However, recent observations of novae in the M31 bulge seem to disprove the evidence of such a "hole" and suggest that the novae too follow the light distribution down to the nucleus (Ciardullo *et al.* 1984).

The "outer bulge" sources could be the remnants of disrupted globular clusters (LVS; see also Grindlay and Hertz 1983). However, Vader *et al.* (1982) have shown that the expected number of such sources is well below the observed value. Most likely these sources result from the evolution of native binary systems (Vader *et al.* 1982). The formation and evolutionary models for such sources are still quite uncertain. The time scale for the formation of low-mass binary X-ray sources could range from a few times 10^9 yr to $\sim 10^{10}$ yr (Rappaport, Joss, and Webbink 1982; Webbink, Rappaport, and Savonije 1983; Taam 1983; Patterson 1984). Therefore they could be related to either the old stellar population or to relatively recent star formation activity. Supporting evidence for the presence of a relatively young population in early-type galaxies comes from the observations of Frogel, Persson, and Cohen (1980). These authors find that the infrared colors of E galaxies could not be explained with the same stellar evolution models that adequately fit the globular cluster data. They tentatively interpret this discrepancy as implying the presence of an intermediate-age population, most likely red supergiants ($1-2 M_\odot$) of a few times 10^9 yr. Such a star formation event could be related to a population of X-ray-emitting binaries only if the initial mass function (IMF) were such as to provide a significant number of native binary systems containing a relatively fast evolving member. Alternatively, X-ray-emitting binaries could evolve from low-mass binary systems that have undergone a Type I supernova event (Gursky 1976; Webbink, Rappaport, and Savonije 1983; Canal, Isern, and Labay 1984). For the latter case, there would be no strong constraint on the age of the original binary system or on the IMF.

Using these models for the formation of low-mass X-ray sources, we can estimate the expected contribution of these sources to the total X-ray luminosity. We expect the integrated X-ray luminosity of the native binary system component to be linearly proportional to the luminous mass of the galaxy, if the gas available for star formation is the result of the mass loss from stars. If all the sources in the outer bulge of M31 are the result of the evolution of such systems into X-ray sources, we can simply scale their number with the total mass. Although this number is an upper limit to the expected number of "native" binary X-ray sources, it is a good estimate of the expected number of sources that were formed through processes that would give a linear relation between integrated X-ray luminosity (or number of sources) and mass (e.g., disrupted globular cluster X-ray sources).

To estimate the number of X-ray sources formed by capture (N_{capture}) we have used the formula in Lightman and Grindlay

TABLE 4
NUMBER OF CAPTURE X-RAY BINARY SOURCES
($L_x = 10^{37}$ ergs s^{-1})

M_T^a (M_\odot)	r_e^a (pc)	r_{capture} (pc)	N_{capture}
3×10^9	150	64	120
3×10^{10}	700	300	80
3×10^{11}	2000	850	184
3×10^{12}	7000	3000	254

^a From Young 1976.

(1982) for sources with $L_x = 10^{37}$ ergs s^{-1} :

$$N_{\text{capture}} \approx 60 \left(\frac{n}{0.01 \text{ pc}^{-3}} \right) \left(\frac{N}{10^{11}} \right) f \left(\frac{\sigma}{250 \text{ km s}^{-1}} \right)^{-1}, \quad (1)$$

where n is the star density, N the number of stars, σ their velocity dispersion, and f the fraction of neutron stars present, which depends on the IMF. Table 4 gives the number of captured X-ray sources N_{capture} estimated as a function of total masses M_T . In order to obtain N_{capture} , we have made the following assumptions:

1. We have taken into account the radial dependence of the quantities in equation (1). To do so, we have used the tables given by Young (1976) for a spherical system that obeys the de Vaucouleurs' $r^{1/4}$ law. For such systems the total mass M_T is related to the effective radius r_e (defined as the radius that contains one-half the total light) by $M_T \propto r_e^2$ (de Vaucouleurs 1958).

2. As shown by equation (1), capture will be most efficient in regions of higher stellar densities and lower stellar velocities (i.e., the innermost regions). We have therefore estimated N_{capture} inside a region of radius r_{capture} , chosen to be a fixed fraction of r_e . In particular, $r_{\text{capture}} \approx 0.44 r_e$. This was obtained assuming $r_{\text{capture}} \approx 400$ pc for a spheroid with $M_T \approx 5 \times 10^{11} M_\odot$ (assumed for the bulge of M31, with $B \approx 5.14$ [de Vaucouleurs 1958] and $M/L = 8.5$ [Faber and Gallagher 1979]), in order to be able to compare our estimates with the bulge of M31. A constant fraction of the total mass is consequently contained within r_{capture} .

3. The free parameter f was chosen to be $f \approx 1 \times 10^{-3}$, in order to reproduce the X-ray observations of the bulge of M31. An average stellar mass $M \approx 0.4 M_\odot$ was assumed for stars.

As can be seen from Table 4, N_{capture} is a very weak function of the total mass M_T . We can explain this by deriving an approximate functional dependence between N_{capture} and M_T . From equation (1) with the above assumptions, we can express N_{capture} as

$$N_{\text{capture}} \approx M_T^2 / \sigma r_e^3. \quad (2)$$

The optical luminosity (hence M_T for constant M/L) is related to σ according to $L_{\text{opt}} \propto \sigma^4$ (Faber and Jackson 1976). Substituting for r_e and σ in equation (2) gives

$$N_{\text{capture}} \approx M_T^{1/4}. \quad (3)$$

Therefore the contribution of captured binary systems to the X-ray luminosity of elliptical galaxies becomes relatively less important in more luminous (massive) galaxies.

iv) Summary

Figure 5 shows the contribution of discrete sources to the X-ray emission of elliptical and S0 galaxies as a function of

optical luminosity (or mass). The contributions of the stellar component, the globular cluster sources, and the native binaries scale linearly with mass. They are normalized at the observations of M31. We have shown above that the number of X-ray binaries formed by "capture" is a function of the mass with a slope $\sim \frac{1}{4}$, and that they contribute very little to the X-ray emission of high-luminosity galaxies. Therefore the integrated X-ray luminosity of various types of individual sources increases almost linearly with the optical luminosity of the galaxies. This means that we can entirely explain the X-ray emission of low-luminosity elliptical galaxies (up to a few times 10^{40} ergs s^{-1}) with the integrated emission of low-mass binaries and globular cluster X-ray sources. However, this component could account for only a few percent of the X-ray luminosity of the more luminous objects. Moreover, the integrated emission of discrete sources fails to explain the steep slope observed between l_x and l_b .

c) Spectra

As discussed above, the two most likely mechanisms for the X-ray emission from normal early-type galaxies are the thermal emission from hot gas and the integrated emission from low-mass binaries, distributed in the galaxy and in globular clusters. A very powerful tool for separating these two components is the spectral signature of the emission. X-ray binary sources show a thermal bremsstrahlung spectrum with characteristic temperatures $\gtrsim 5$ keV (e.g., van den Heuvel 1980). The same spectrum is observed in globular cluster sources (Hertz and Grindlay 1983). The X-ray emission from hot gas should instead be characterized by a much softer spectrum, with $kT \lesssim 1$ keV, as estimated by White and Chevalier (1984). The X-ray observations of the high-mass galaxy M87 show that the gas is at a temperature of a few keV in the outer regions but decreases to ~ 1 keV in the region within a $3'$ radius from the nucleus (Fabricant and Gorenstein 1983).

The X-ray spectra available for some of the elliptical and S0 galaxies show temperatures of the order of 1 keV (Stanger and Schwarz 1984; Forman, Jones, and Tucker 1985; Nulsen, Stewart, and Fabian 1984). This would favor the hot gas emission over the binary and globular cluster source emission in early-type galaxies. However, the spectra were only derived for the high-luminosity objects ($l_x \gtrsim 10^{23}$ ergs s^{-1} Hz^{-1}). In these galaxies the hot gas is indeed likely to dominate the X-ray emission.

d) The Onset of Nuclear Activity in Elliptical Galaxies

The detailed observations of a few normal elliptical and S0 galaxies (Nulsen, Stewart, and Fabian 1984; Stanger and Schwarz 1984; Forman, Jones, and Tucker 1985) show that the X-ray emission of the more luminous objects is extended on a scale comparable to or larger than the optical extent. This evidence excludes the possibility that the bulk of the X-ray emission in normal early-type galaxies is due a nuclear source. With the present data we cannot directly isolate and study weak nuclear X-ray emission in these galaxies. To study the onset and the effect of X-ray nuclear activity in elliptical galaxies, we can compare the present sample with the sample of bright elliptical galaxies associated with strong 3CR radio sources studied by Fabbiano *et al.* (1984). 3CR galaxies are X-ray sources with L_x in the range 10^{42} – 10^{45} ergs s^{-1} , and their X-ray luminosity is well correlated with their nuclear

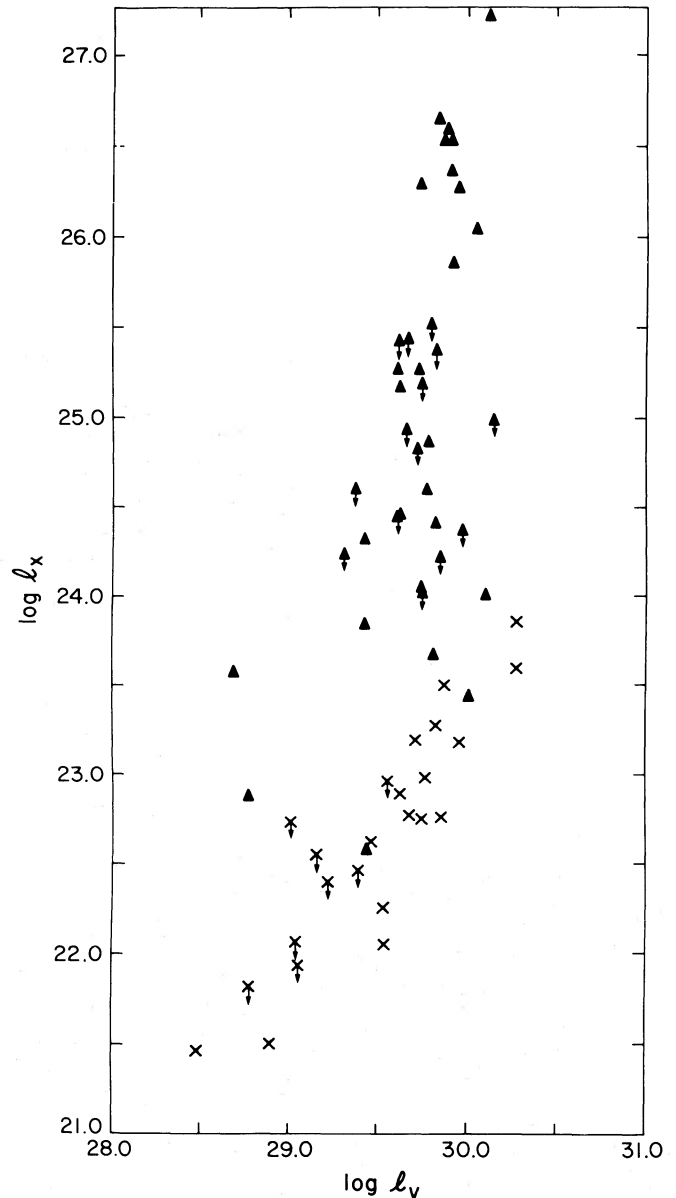


FIG. 6.—The monochromatic X-ray luminosity is plotted against the optical luminosity for normal elliptical and S0 galaxies (this sample, crosses) and the 3CR galaxies (Fabbiano *et al.* 1984, triangles). The V -band magnitudes have been used for consistency with the data for 3CR galaxies.

radio power, and often with emission line features, thus suggesting a nuclear origin for the X-ray emission.

The monochromatic X-ray and optical luminosities of the 3CR galaxies from Fabbiano *et al.* (1984) and of the normal galaxies from this sample are shown in Figure 6. The 3CR galaxies follow the general trend between X-ray and optical luminosity found for normal galaxies, but are systematically displaced toward higher X-ray luminosities, although with some overlap at $l_x \approx 10^{23}$ – 10^{24} ergs s^{-1} Hz^{-1} . In particular, the higher X-ray luminosity objects show a very steep relation of X-ray to optical luminosity. With a linear regression analysis (see § III) applied to the high-X-ray-luminosity ($l_x \geq 10^{25}$ ergs s^{-1} Hz^{-1}) 3CR galaxies, we find: $\log l_x = (4.0 \pm 0.1) \log l_v - 93.74$, with a 99% confidence region for the slope

between 1.85 and 6.0. This is significantly steeper than that found for normal early-type galaxies (see Table 3).

The high-X-ray-luminosity galaxies are also optically bright ($l_v > 2 \times 10^{29}$ ergs s⁻¹ Hz⁻¹). This would suggest that high luminosity is necessary for the onset of a powerful nuclear source. However, it is evident from Figure 6 that this is not sufficient to ensure nuclear activity, since normal and active (3CR) galaxies are in the same range of optical luminosity. Two parameters, mass and ellipticity, have been suggested to govern the onset of radio activity in elliptical galaxies (Heckman 1983; Heeschen 1970; Hummel, Kotanyi, and Ekers 1983). A critical mass might be needed to retain enough gas to fuel the nuclear engine (see Norman and Silk 1979). Even optically bright but radio-quiet galaxies may have this critical mass, since a substantial amount of their interstellar gas is visible at X-ray temperatures at the present time (see above). Ellipticity might be the critical parameter that regulates the accretion onto the nuclear source (Hummel, Kotanyi, and Ekers 1983) and the onset of nuclear activity in radio-loud galaxies. These are two independent quantities, since massive galaxies do not tend to be rounder than less massive ones (see Davies *et al.* 1983; Tonry and Davis 1981).

It would then follow that the X-ray-luminous 3CR galaxies are round and massive systems, where the gas is continuously accreting onto the nucleus and is powering a central (radio and X-ray) source. This central source sustains a powerful extended radio source (most often a classical double) and dominates the emission in X-rays. Similar conclusions are reached by Dressel and Wilson (1985) from the study of the X-ray emission from a

small sample of early-type galaxies with compact nuclear radio sources. The 3CR galaxies with $l_x < 10^{25}$ ergs s⁻¹ Hz⁻¹ could be massive but flatter systems (or round but less massive ones). Their nuclear sources do not dominate their X-ray emission, which thus becomes similar to that of normal radio-quiet early-type galaxies of similar high optical luminosity. The latter might be flatter and less massive systems, where the importance of the central sources has become negligible.

The above scenario, however, cannot account for the very steep dependence of the X-ray luminosity on the optical luminosity for X-ray luminous 3CR galaxies. If we regard these latter as having X-ray-optical properties intermediate between galaxies and quasars, we might be able to understand this steep relation. Tananbaum *et al.* (1983) have studied a sample of 3CR quasars observed in X-rays and found that for these objects, $l_x \propto l_o^{0.5}$. An exponent of ~ 0.7 is obtained by Zamorani (1982) for a more heterogeneous sample of radio-loud quasars. The optical and X-ray luminosities for the 3CR galaxies and 3CR quasars are shown in Figure 7. A power-law exponent of 0.5–0.8 for the quasar sample can be explained in terms of accretion models at a rate near the Eddington limit (see Tucker 1983). In these models, the optical luminosity refers to the luminosity of the region where the X-rays originate. In 3CR galaxies, however, the optical emission is probably dominated by the parent galaxy, while the nuclear region is most likely what we observe in quasars. The extrapolation of the X-ray-optical correlation for quasars to lower luminosities (see Fig. 7) shows that while the X-ray emission from the nucleus would still be dominant, its expected optical lumin-

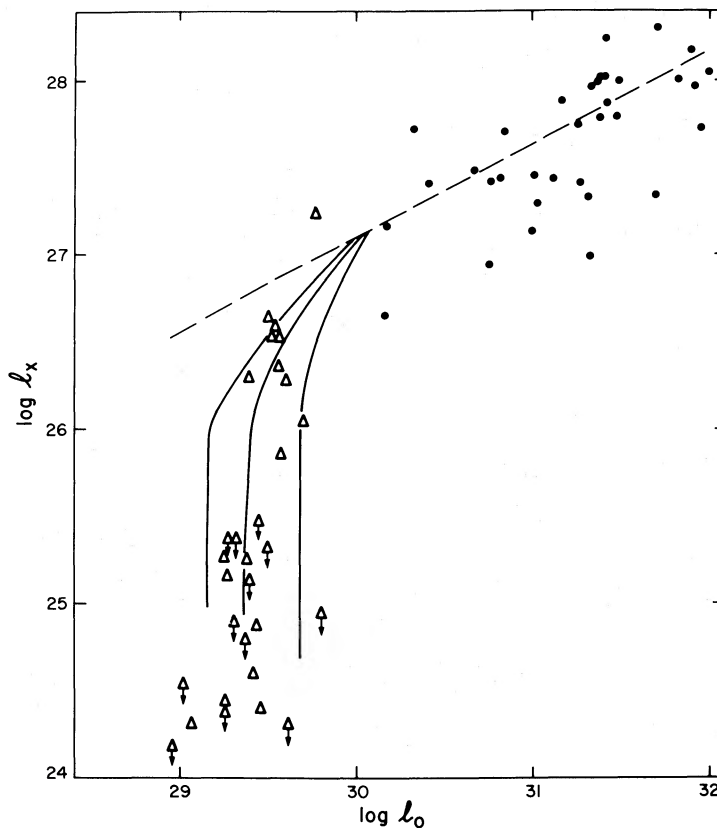


FIG. 7.—The monochromatic X-ray luminosity of 3CR quasars (Tananbaum *et al.* 1983, circles) and 3CR galaxies (Fabbiano *et al.* 1984, triangles) plotted as a function of optical luminosity (as defined in Zamorani *et al.* 1981). The dashed line represents the best fit to the 3CR quasar data. The solid lines represent how this best fit is modified when the effect of the whole galaxy is considered for three different optical luminosities.

osity would give a marginal contribution to the total optical emission for $l_x \lesssim 10^{26}$ ergs s⁻¹ Hz⁻¹. Adding the parent galaxy contribution to the nuclear emission changes the optical luminosity substantially, but not the X-ray luminosity. In Figure 7, we show this effect. The curves plotted are obtained by adding the total optical luminosity of the galaxy (for three choices of l_0) to the optical luminosity of the nucleus as predicted from the correlation observed in radio-loud quasars. Since the total galaxy dominates in the optical when the X-ray luminosity is $l_x \lesssim 10^{26}$ ergs s⁻¹ Hz⁻¹, the resulting curves are almost independent of the observed total optical luminosity. As shown in Figure 7, this could give a reasonable explanation of the steep X-ray–optical correlation in X-ray luminous 3CR galaxies.

V. SUMMARY AND CONCLUSIONS

We have shown that in early-type galaxies the X-ray luminosity l_x is correlated with the optical (blue) luminosity l_B . This correlation is significantly steeper than that observed for late-type galaxies: $l_x \propto l_B^{1.64 \pm 0.15}$ for the elliptical and S0 galaxy sample, while $l_x \propto l_B^{1.08 \pm 0.07}$ for spirals and irregulars (FT). The difference between these two relations is significant at the 99.99% confidence level. This result suggests a different origin of the X-ray emission in early-type galaxies.

There seem to be two separate mechanisms for the X-ray emission in high-luminosity and low-luminosity objects: thermal emission from hot gas is most likely responsible for the emission in galaxies with $L_x \gtrsim 10^{41}$ ergs s⁻¹, while low-mass binary sources dominate in galaxies with $L_x \lesssim 10^{40}$ ergs s⁻¹. There is some evidence to support the hot gas origin. The X-ray spectra of a few high-luminosity objects are too soft for low-mass binary sources but are consistent with a thermal emission of gas at $\sim 10^7$ K. The detailed observations of a few objects, namely, M84 and M86, are consistent with hot gas emission. However, this hot gas component cannot dominate in low-luminosity objects, as shown by the observations of the bulge of M31 and possibly of M32, where compact sources dominate. In low-luminosity objects the X-ray emission can be accounted for by a collection of globular cluster and low-mass

binary sources. Similar tentative conclusions have been reached by Stanger and Schwarz (1984) based on a smaller sample of early-type galaxies. This indicates that a critical galaxy mass might be needed to retain a large amount of hot gas (see Norman and Silk 1979).

The power-law exponent of the $l_x - l_B$ relation was derived assuming that a single law could represent the data. However, it is most likely that two separate relations of l_x to l_B are needed. We expect a linear relationship between l_x and l_B at low optical and X-ray luminosities; at high luminosities, both a steep dependence of l_x on l_B , such as that expected from the hot coronae model (Forman, Jones, and Tucker 1985), or from gravitational cooling flows (Nulsen, Stewart, and Fabian 1984). They could also be consistent with a linear dependence truncated below $l_B \approx 2 \times 10^{29}$ ergs s⁻¹ Hz⁻¹, if cooling flows with a significant supernova energy input occur (White and Chevalier 1984). For a mass-to-light ratio $M/L = 10$, this corresponds to a galaxy mass $M \approx 5 \times 10^{11} M_\odot$.

The extended X-ray emission of radio-quiet galaxies (Stanger and Schwarz 1984; Forman, Jones, and Tucker 1985; Nulsen, Stewart, and Fabian 1984) is qualitatively different from the emission observed in radio-loud galaxies of the same optical luminosity (3CR galaxies), where the X-ray emission is much stronger and is most likely of nuclear origin (Fabbiano *et al.* 1984). In particular, the 3CR galaxies can be regarded, in their X-ray properties, as an extension at lower luminosities of quasars of similar radio properties (3CR sample, Tananbaum *et al.* 1983). The high optical luminosity, or possibly the high mass (Heckman 1983), is most likely a necessary, but not sufficient, condition for the onset of a powerful nuclear X-ray source in early-type galaxies. In analogy to what has been suggested for the radio nuclear activity (Hummel, Kotanyi, and Ekers 1983), the galaxy ellipticity might influence the nuclear activity in X-rays.

We thank J. Schwarz, W. Tucker, M. Elvis, G. Zamorani, and J. Stocke for useful discussions. This work was supported under NASA contract NAS8-30751.

REFERENCES

- Aaronson, M. 1977, Ph.D. thesis, Harvard University.
 Avni, Y. 1984, in preparation.
 Avni, Y., Soltan, A., Tananbaum, H., and Zamorani, G. 1980, *Ap. J.*, **238**, 800.
 Bechtold, J., Forman, W., Giacconi, R., Jones, C., Schwarz, J., Tucker, W., and Van Speybroeck, L. 1983, *Ap. J.*, **265**, 26.
 Biermann, P., and Kronberg, P. P. 1983, *Ap. J. (Letters)*, **268**, L69.
 Canal, R., Isern, I., and Labay, J. 1984, *Proc. X-Ray Symposium (Bologna)*, ed. M. Oda and R. Giacconi (Tokyo: Institute of Space and Astronomical Science), p. 293.
 Ciardullo, R., Ford, H. C., Jacoby, G., Neill, J. D., and Shafter, A. 1984, *Bull. AAS*, **16**, 977.
 Davies, R. L., Efstathiou, G., Fall, S. N., Illingworth, G., and Schechter, P. L. 1983, *Ap. J.*, **266**, 41.
 de Vaucouleurs, G. 1958, *Ap. J.*, **128**, 465.
 de Vaucouleurs, G., de Vaucouleurs, A., and Corwin, H. G. 1976, *Second Reference Catalog of Bright Galaxies* (Austin: University of Texas Press).
 Dressel, L. L., and Condon, J. 1978, *Ap. J. Suppl.*, **36**, 53.
 Dressel, L. L., and Wilson, A. 1985, *Ap. J.*, **291**, 668.
 Fabbiano, G., Miller, L., Trinchieri, G., Elvis, M., and Longair, M. 1984, *Ap. J.*, **277**, 115.
 Fabbiano, G., Trinchieri, G., and Macdonald, A. 1984, *Ap. J.*, **284**, 65.
 Fabbiano, G., and Trinchieri, G. 1985, *Ap. J.*, **296**, 430 (FT).
 Faber, S. M. 1973, *Ap. J.*, **179**, 731.
 ———, 1981, in *Astrophysical Cosmology: Proceedings of the Vatican Study Week on Cosmology and Fundamental Physics*, ed. H. A. Brück, G. V. Coyne, and M. S. Longair (Rome: Specola Vaticana), p. 219.
 Faber, S. M., and Gallagher, J. 1976, *Ap. J.*, **204**, 365.
 ———, 1979, *Ann. Rev. Astr. Ap.*, **17**, 135.
 Faber, S. M., and Jackson, R. E. 1976, *Ap. J.*, **204**, 688.
 Fabricant, D., and Gorenstein, P. 1983, *Ap. J.*, **267**, 535.
 Feigelson, E. D., Schreier, E. J., Delvaile, J. P., Giacconi, R., Grindlay, J. E., and Lightman, A. P. 1981, *Ap. J.*, **251**, 31.
 Forman, W., Jones, C., and Tucker, W. 1984, in *Clusters and Groups of Galaxies*, ed. F. Merdrossian, G. Giuricin, and M. Mezzetti (Dordrecht: Reidel), p. 297.
 ———, 1985, *Ap. J.*, **293**, 102.
 Frogel, J. A., Persson, S. E., Aaronson, M., Becklin, E. E., Mathews, K., and Neugebauer, G. 1975a, *Ap. J. (Letters)*, **195**, L15.
 ———, 1975b, *Ap. J. (Letters)*, **200**, L123.
 Frogel, J. A., Persson, S. E., and Cohen, J. G. 1980, *Ap. J.*, **240**, 785.
 Grindlay, J. E., and Hertz, P. 1983, in *Cataclysmic Variables and Low Emission X-Ray Binaries*, ed. D. Q. Lamb and J. Patterson (Dordrecht: Reidel), p. 79.
 Gunn, J. E., Stryker, L. L., and Tinsley, B. M. 1981, *Ap. J.*, **249**, 48.
 Gursky, H. 1976, in *IAU Symposium 73, Structure and Evolution of Close Binary Systems*, ed. P. Eggleton, S. Mitton, and J. Whelan (Dordrecht: Reidel), p. 19.
 Harnett, I. J. 1982, *Australian J. Phys.*, **35**, 321.
 Harris, W. E., and Racine, R. 1979, *Ann. Rev. Astr. Ap.*, **17**, 241.
 Heckman, T. M. 1983, *Ap. J.*, **273**, 505.
 Heeschen, D. S. 1970, *A.J.*, **75**, 523.
 Hertz, P., and Grindlay, J. E. 1983, *Ap. J.*, **275**, 105.
 Hummel, E. 1980, *Astr. Ap.*, **106**, 183.
 Hummel, E., Kotanyi, C. G., and Ekers, R. D. 1983, *Astr. Ap.*, **127**, 205.
 Larson, R. B., and Tinsley, B. M. 1974, *Ap. J.*, **192**, 293.
 ———, 1978, *Ap. J.*, **219**, 46.
 Lightman, A. P., and Grindlay, J. E. 1982, *Ap. J.*, **262**, 145.

- Long, K. S., and Van Speybroeck, L. 1983, in *Accretion Driven X-Ray Sources*, ed. W. Lewin and E. P. J. van den Heuvel (Cambridge: Cambridge University Press), p. 41 (LVS).
- Mathews, W. G., and Baker, J. C. 1971, *Ap. J.*, **170**, 241.
- Norman, C., and Silk, J. 1979, *Ap. J. (Letters)*, **233**, L1.
- Nulsen, P. E. J., Stewart, G. C., and Fabian, A. C. 1984, *M.N.R.A.S.*, **208**, 185.
- Patterson, J. 1984, *Ap. J. Suppl.*, **54**, 443.
- Persson, S. E., Frogel, J. A., and Aaronson, M. 1979, *Ap. J. Suppl.*, **39**, 61.
- Rappaport, S., Joss, P. G., Webbink, R. F. 1982, *Ap. J.*, **254**, 616.
- Rosino, L. 1973, *Astr. Ap. Suppl.*, **9**, 347.
- Sanders, R. H. 1981, *Ap. J.*, **244**, 820.
- Schmitt, J. H. M. M. 1985, *Ap. J.*, **293**, 178.
- Stanger, V., and Schwarz, J. 1984, preprint.
- Taam, R. E. 1983, *Ap. J.*, **270**, 694.
- Tananbaum, H., Wardle, J., Zamorani, G., and Avni, Y. 1983, *Ap. J.*, **268**, 60.
- Tonry, J. L., and Davis, M. 1981, *Ap. J.*, **246**, 680.
- Trinchieri, G., Fabbiano, G., and Palumbo, G. G. C. 1985, *Ap. J.*, **290**, 96.
- Tucker, W. 1983, *Ap. J.*, **271**, 531.
- Vader, J. P., van den Heuvel, E. P. J., Lewin, W. H. G., and Takens, R. J. 1982, *Astr. Ap.*, **113**, 328.
- van den Bergh, S. 1975, *Ann. Rev. Astr. Ap.*, **13**, 217.
- van den Heuvel, E. P. J. 1980, in *X-Ray Astronomy, Proc. NATO Advanced Study Institute* (Erice, Sicily, 1979 July 1-14), ed. R. Giacconi and G. Setti (Dordrecht: Reidel), p. 119.
- Van Speybroeck, L., and Bechtold, J. 1981, in *X-Ray Astronomy with the Einstein Satellite*, p. 153.
- Van Speybroeck, L., Epstein, A., Forman, W., Giacconi, R., Jones, C., Liller, W., and Smarr, L. 1979, *Ap. J. (Letters)*, **234**, L45.
- Webbink, R. F., Rappaport, S., and Savonije, G. J. 1983, *Ap. J.*, **270**, 678.
- White, R. E., and Chevalier, R. A. 1984, *Ap. J.*, **280**, 561.
- Young, P. I. 1976, *A.J.*, **81**, 807.
- Zamorani, G. 1982, *Progress in Cosmology, Proc. Oxford International Symposium*, ed. A. W. Wolfendale (Dordrecht: Reidel), p. 203.
- Zamorani, G., et al. 1981, *Ap. J.*, **245**, 357.

G. TRINCHIERI and G. FABBIANO: High Energy Astrophysics Division, Center for Astrophysics, 60 Garden Street, Cambridge, MA 02138